

A REACTION-DIFFUSION SYSTEM WITH PERIODIC FRONT DYNAMICS*

GEORGIY S. MEDVEDEV[†], TASSO J. KAPER[†], AND NANCY KOPELL[†]

Abstract. A reaction-diffusion model motivated by *Proteus mirabilis* swarm colony development is presented and analyzed in this work. The principal variables are the concentrations of swarm cells and swimmer cells, which are multicellular and single-cell forms, respectively, of the *Proteus mirabilis* bacteria. The kinetic terms model the growth and division process of the swimmer cells, as well as the formation and septation of swarm cells. In addition, a nonlinear diffusion is employed for the swarm cell migration that incorporates several essential aspects of the concentration-dependent dynamics observed in experiments.

The model exhibits time-periodic colony evolution in which each period consists of two distinct phases: a swarming phase and a consolidation phase. Both are very similar to those seen in experiments. During the swarming phase, the colony expands as swarm cells migrate outward to form a new terrace beyond the colony's initial boundary. Gradually, this expansion slows down and stops, and then the consolidation phase begins, during which time the colony boundary stays in place, but the swarm and swimmer concentrations inside the colony boundary change significantly. Finally, when the swarm cell concentration has reached a threshold, the consolidation phase ends abruptly and the next swarming phase begins, repeating the cycle.

We analyze both of these phases, as well as the transitions and switches (gradual and abrupt) between them, using the method of matched asymptotic expansions and theory for parabolic partial differential equations. We show that the dynamics of the diffusivity play a central role in determining the colony evolution during the consolidation phase and in the occurrence of an abrupt transition to the subsequent swarming phase. In particular, we show that the diffusivity profile forms a wave that propagates behind the front toward the colony boundary. It grows sharply in amplitude and forms a spike when it reaches the boundary. Moreover, it is precisely this event that triggers swarming. Analysis of the diffusivity dynamics also leads to an understanding of the swarming phase dynamics and the gradual transition to the consolidation phase that follows it. These analyses show that the concentrations at the beginning of the two phases naturally repeat in a time-periodic manner. Finally, we present rigorous estimates for the inner and outer solutions developed in the matched asymptotic analysis, and for their domains of validity.

Key words. reaction-diffusion systems, *Proteus mirabilis* bacterial colonies, population dynamics, interface dynamics, matched asymptotic analysis

AMS subject classifications. 35Q80, 35K57, 35K65, 92D25

PII. S0036139998344635

1. Introduction. Systems of nonlinear parabolic partial differential equations (PDEs), or reaction-diffusion systems, have long been a subject of active research. These systems have numerous applications in physics, chemistry, ecology, biology, and other disciplines. Examples include problems in combustion, phase transitions, formation of patterns in chemical reactions and living systems, propagation of electrical signals in nerve axons and cardiac tissue, population dynamics, cellular differentiation, and morphogenesis, to name a few. It is beyond the scope of this paper to give a review of the theory and applications of reaction-diffusion systems. For systematic

*Received by the editors September 14, 1998; accepted for publication (in revised form) April 25, 1999; published electronically May 15, 2000. The research of the first and second authors was partially supported by National Science Foundation grant DMS-9624471. The research of the first and third authors was partially supported by National Science Foundation grant DMS-9706694. The research of the second author was partially supported by the Alfred P. Sloan Foundation.

<http://www.siam.org/journals/siap/60-5/34463.html>

[†]Department of Mathematics and Center for BioDynamics, Boston University, Boston, MA 02215 (medvedev@math.bu.edu, tasso@math.bu.edu, nk@math.bu.edu).

expositions of some aspects of the theory, numerous applications, and a comprehensive list of literature on this subject we refer to [4, 9, 23, 27, 30].

Reaction-diffusion systems have also been used extensively in studies of self-organization, development, and pattern formation principles in bacterial colonies [3, 5, 16]. For example, there is a large body of literature devoted to the mathematical modeling of aggregating *Dictyostellium* amoeba [17, 14, 15]. Another important example is provided by *Proteus mirabilis* swarm colony development [8]. The salient feature of the *Proteus mirabilis* colonies is the periodic character of their morphogenesis. These colonies undergo alternating phases of migration over the substrate and growth without change of the colony boundaries. These phases are called the swarming and consolidation phases, respectively. The study of the swarming phenomenon in *Proteus mirabilis* bacterial colonies has a long and exciting history. In the present paper, we give the minimal biological information necessary for understanding of our modeling objectives and assumptions. The detailed biological and biophysical descriptions of the swarming phenomenon can be found in [2, 24, 25, 28].

The goal of the mathematical modeling of the *Proteus mirabilis* colonies is to study the dynamics of the individual phases, to determine the switching mechanisms and transitions between the phases, and to shed some light on the sources of their time-periodic alternation.

In the present paper, we study a mathematical model motivated by the *Proteus mirabilis* swarm colony development,

$$(1.1) \quad \begin{aligned} u_t(x, t) &= \nu v(x, t) + (\alpha - \mu) u(x, t) + (D(u, v) u_x(x, t))_x, \\ v_t(x, t) &= (\alpha - \nu) v(x, t) + \mu u(x, t), \end{aligned}$$

with appropriate compactly supported initial conditions. The unknown functions, $u(x, t)$ and $v(x, t)$, correspond to the surface densities of the populations of *swarm* cells and *swimmer* cells, respectively, which are the multicellular and single-cellular forms of the bacteria encountered in the colony. The density-dependent functions α , μ , and ν characterize the cellular growth, division, and differentiation that constitute the kinetic part of the system. Finally, the swarm cell migration is modeled by the nonlinear diffusion term in (1.1), whereas the swimmer cells do not appear to move, and hence the second equation does not contain any spatial derivatives.

The nonlinear form of the diffusion coefficient

$$(1.2) \quad D(u, v) = \frac{D_0 u}{u + kv}$$

is an essential ingredient in our model. Whereas random migration is usually modeled by the Laplace operator, there are often factors in problems of population dynamics that can give some bias to certain directions of migration, e.g., migration to avoid crowding. These factors lead to the diffusion coefficient being density dependent. A central aspect to modeling *Proteus mirabilis* colonies is that only a part of the population, the swarm cells, appear to move. The presence of the swimmer cells, in contrast, slows down the rate of migration, since they form obstacles in the way of moving swarm cells. In addition, the biological descriptions in [28] suggest that swarming is a cooperative process. For example, it is reported therein that movement of individual cells seems to be retarded, whereas cells moving in larger groups do so more effectively. Also according to [25], colony expansion involves multicellular *rafts* of swarm cells. Hence, we assume that the probability of forming these rafts is higher (and, therefore, so is diffusivity) in the areas with a higher proportion of swarm

cells in the total cell population. Therefore, the diffusion coefficient can be modeled as a weighted ratio of the swarm cell population density to the density of the total population at a given point, as given by (1.2).

The functions $u(x, t)$ and $v(x, t)$ stay compactly supported for all finite times, due to the nonlinearity of D in (1.2), provided the initial data have compact support. Therefore, the position of the colony boundary, or interface, is well defined.

Mathematically, the most interesting feature of the system (1.1) and (1.2) is that it generates interface dynamics that are time periodic, just as seen in the experiments of [25, 26, 28] and in the Esipov–Shapiro model [8]. Numerical simulations of (1.1) show that the colony evolves in alternating phases of swarming and consolidation. A swarming phase is characterized by expansion in the colony radius that is rapid at first with an apparently constant velocity and that gradually slows down until the colony boundary stops advancing. In this way a new terrace is developed at the outer rim of the colony during a swarming phase. The consolidation phase, which begins immediately after completion of the preceding swarming phase, is then identified as the time interval during which the colony boundary stays fixed, but during which there is significant increase in the concentrations of swimmer and swarm cells in the new terrace behind the front. (See Figure 1.) Moreover, from the numerical simulations, it is observed that the u, v concentration profiles at the end of the consolidation phase are nearly identical (but translated) to the profiles at the beginning of the preceding swarming phase. Hence, the alternating of swarming and consolidation continues in a time-periodic manner.

The dynamics of the diffusion coefficient play a central role in the analysis of both phases, and we begin by describing the consolidation phase. During the consolidation phase, the diffusion coefficient exhibits interesting dynamics in the region behind the front. Numerically, we have found that the dynamics of the diffusion coefficient resemble a front traveling in the outward radial direction. When this front catches up with the colony boundary, the spatial distribution of the diffusion coefficient in the vicinity of the colony boundary changes drastically; it takes the form of a spike. The appearance of the spike profile of the diffusivity corresponds to the switch from the consolidation to swarming. It is the most signal event of the whole cycle.

We show that these dynamics can be understood by studying the interaction of the wave of diffusivity and the colony boundary. Unfortunately, analyzing this phenomenon using the system (1.1) appears to be far from trivial, since one must solve an initial value problem (IVP) for a system of two nonlinear equations. However, we have managed to reproduce and to study the switch of the consolidation and swarming phases using only a scalar reaction-diffusion equation:

$$(1.3) \quad z_t(x, t) = z(1 - z) + \frac{1}{v} (D(z) (vz)_{xx}), \quad \mu > 0,$$

where

$$v(x) \equiv \frac{A + \alpha}{2} - \frac{A - \alpha}{2} \tanh\left(\frac{x - x^*}{\epsilon}\right), \quad 0 < \alpha < A, \quad 0 < \epsilon \ll 1.$$

Here, $v(x)$ plays a role of a static approximation of the $v(x, t)$ in (1.1) in the neighborhood of the colony boundary x^* at the end of the consolidation phase. Already with $D(z) \equiv 1$, the numerics for (1.3) show a high degree of similarity between the solution dynamics of the full system (1.1) and that of the reduced one (1.3) (Figure 5). This similarity becomes even more pronounced when numerically solving (1.3) with $D(z)$ given by (1.2) (Figure 6).

We start by carrying out a formal matched asymptotics analysis for the solution of an IVP for (1.3) with $D(z) \equiv 1$. Next, we show that this analysis can be extended to study (1.3) with nonlinear diffusion coefficients $D(z)$. Moreover, in the $O(\epsilon)$ -wide transition layer about x^* we obtain, up to an exponentially small error, an analytical solution of the IVP for (1.3). It explains the mechanism for the generation of the spike profile of z in the transition layer. We argue that the same mechanism is involved in the generation of the spike profile of the diffusivity in the full system (1.1), and we also comment on the relation between the full problem (1.1) and the reduced one (1.3).

Justifying the use of matched asymptotics in reaction-diffusion systems is often a difficult task, in spite of a long history of work [7, 10, 11, 20, 29] in this area and a wide range of applications. In our case, we obtain the detailed estimates of the error made when the exact solution is approximated by the asymptotic one. In particular, we estimate the maximal sizes of the spatial domains where these estimates hold, and we show that the method gives approximate solutions that are uniformly valid in time for the IVP (1.3) on bounded sets of the real line.

Understanding the behavior of the solution immediately before the end of the consolidation phase is important for the understanding of the dynamics of the subsequent swarming phase as well. The spatial distributions of the concentrations at the end of the consolidation phase serve as initial conditions for the IVP that describes the swarming phase. From this IVP, we can infer that the diffusivity and, hence, the rate of colony expansion reach their maximum values at the start of the swarming phase. Finally, throughout the swarming phase, the diffusivity gradually decreases until the interface comes almost to a rest. Then numerical solution shows that u , v , D profiles are the same as they were at the beginning of the preceding consolidation phase and the whole cycle begins again.

The formation of spatial patterns in *Proteus* colonies was first mathematically modeled by Esipov and Shapiro in [8], and additional analysis has been carried out in [1]. In the Esipov–Shapiro model, not only are the time and space variables, but another independent variable, the age of a swarm cell, is introduced to account for the swarm cell evolution. The general framework of the problems for age-structured populations with diffusion is given, e.g., in [13]. The age-dependence of the key parameters, including the diffusion coefficient, is an important ingredient of the Esipov–Shapiro model. In particular, they compare two variants of the model, Model A and Model B. The Model A exhibits a more pronounced age-dependence and the results of numerical studies show that Model A also gives rise to more pronounced periodicity of the colony evolution.

Our work can be viewed as a continuation of studies of the modeling of the *Proteus* colonies initiated in [8]. We start out with the same simplified assumptions on the colony morphogenesis that correspond to the kinetic part (without diffusion) of the Esipov–Shapiro model. We show that these two kinetic models result in the same large time dynamics, which have an attracting fixed point for the ratio of the swarm cell and swimmer cell population densities. When formulating the problem with diffusion, our main hypothesis is that the main colony development characteristics are density-dependent, rather than dependent on the age-structure of the swarm cell population, as was assumed in [8]. With the parameters α , ν , μ , and D not depending explicitly on the age variable, one can transform Model A into B via averaging the dependent functions u and v over the age structure. We show that even a simpler Model B exhibits robust periodicity of the colony expansions.

The rest of the paper is organized as follows. In section 2, we state the modeling assumptions on the colony morphogenesis and formulate the kinetic part of the model. The analysis of the kinetic equations and the time-asymptotic properties of its solutions follows in section 3. In section 4, we extend the model to account for the swarm cell migration. This results in a system of a parabolic PDE coupled with an ordinary differential equation (ODE) (1.1)–(1.2). We study this system numerically in section 5. The results show periodic colony expansions. In section 6, we focus on the dynamics of the consolidation phase. In particular, we construct the asymptotic procedure to analyze the dynamics of the diffusion coefficient in the neighborhood of the colony boundary. This explains the generation of the spike profile of diffusivity—the culmination of the dynamics of the consolidation phase. In section 7, we turn to study the swarming phase. Sections 8 and 9 contain the full justification of the asymptotic procedure developed in section 6.

2. The equations of local kinetics. In this section, we state our modeling assumptions on the *Proteus mirabilis* morphogenesis and derive equations of local kinetics, following [8].

First, we assume that the colony consists of cells of two types: swarm cells and swimmer cells, which are the unicellular and multicellular forms, respectively. We denote by $v(t)$ the number of swimmer cells per unit area, i.e., the density of the swimmer cell population. The number of swarm cells of age $a > 0$ per unit area is denoted by $q(t, a)$.

We consider the following model of the local colony development [8]:

$$(2.1) \quad q_t(t, a) + q_a(t, a) = -\mu(a)q(t, a),$$

$$(2.2) \quad v'(t) = \frac{1 - \xi}{\tau}v(t) + \int_0^t \mu(a)q(t, a)e^{\frac{a}{\tau}} da, \quad t > 0, \quad a > 0.$$

Equation (2.1) is a typical equation of evolution of an age-structured population [13]. A nonnegative function $\mu(a)$, the rate of mortality, is discussed below along with assumptions on swarm cell mortality, or *separation*.

Equation (2.2) describes the evolution of the swimmer cell population. The first term on the right accounts for the fact that of all swimmer cells present at any given instant of time, a fraction, $1 - \xi$, goes through the normal growth and division cycle. Specifically, the rate of change of the number of swimmer cells is directly proportional to the number of swimmer cells present, with rate constant equal to τ^{-1} . The constant ξ is called a differentiation factor. The second term in (2.2) comes from swimmer cells that are created by *separation* of swarm cells, i.e., division of these cells in several places to form smaller swimmer cells. To understand the form of this term, we note that the fraction, ξ , of swimmer cells enters the swarm cell development channel. Thus, the swarm cell birth law is given by

$$(2.3) \quad q(t, 0) = \frac{\xi}{\tau}v(t).$$

The factor τ^{-1} on matches the dimensions of two sides of (2.3). We recall that $q(t, a)$ is the number of swarm cells per unit area and per unit age, whereas $v(t)$ is the number of cells per unit area only.

Once a swarm cell has been created, its length grows exponentially, with the same rate constant equal to τ^{-1} . Hence, at the age a a swarm cell is $e^{\frac{a}{\tau}}$ times larger than

its parent swimmer cell. In (2.1)–(2.2), $\mu(a)da$ represents, for a swarm cell of age a , the probability of dying, or septating (i.e., dividing in several places along its body to produce swimmer cells). Accordingly, the second term on the right-hand side of (2.2) represents an instantaneous rate of change in the swimmer cell population due to swarm cell septation.

Remark. In the present and following sections we have assumed that τ^{-1} and ξ are constants. However, in section 4 we shall define the rate of growth and the differentiation factor as piecewise constant functions of the cell population densities.

It remains to specify the modeling assumptions on the rate of septation $\mu(a)$. Following [8], we consider two models based on the assumptions: the septation of a swarm cell occurs, when it has reached

(Model A) a certain fixed age, Θ ; or

(Model B) a random age, chosen from the uniform distribution on $[0, \Theta]$.

Therefore, in (2.1)–(2.2), we have

$$(2.4) \quad \mu(a) = \begin{cases} \delta(a - \Theta), & \text{Model A,} \\ \Theta^{-1}\chi_{(0, \Theta)}(a), & \text{Model B,} \end{cases}$$

where $\chi_{(0, \Theta)}(\cdot)$ denotes the characteristic function for $(0, \Theta)$, and $\delta(\cdot)$ is the Dirac delta function. In the definition above and throughout this paper we adopt the following convention:

$$(2.5) \quad \int_{-\infty}^0 \delta(x)dx = 0.$$

We conclude this section by identifying a third important dependent variable, namely swarm cell population density. As we already noted, a swarm cell of age a is $e^{\frac{a}{\tau}}$ times longer than its parent swimmer cell. Assuming that a swimmer cell has a unit mass per unit length, the age-dependent density of the swarm cell population is $q(t, a)e^{\frac{a}{\tau}}$. Integrating over all ages, we obtain the swarm cell population density

$$(2.6) \quad u(t) = \int_0^{\infty} q(t, a)e^{\frac{a}{\tau}} da.$$

We shall find this quantity useful in analyzing the kinetics of both models in the next section, as well as for the diffusion problem to be introduced in section 4.

Remark. With the assumptions we have made on the mechanism of septation in both models, all swarm cells septate with probability 1 by the age of Θ . Therefore,

$$(2.7) \quad q(t, a) = 0 \quad \text{for } a > \Theta,$$

and (2.6) can be rewritten as

$$(2.8) \quad u(t) = \int_0^{\Theta} q(t, a)e^{\frac{a}{\tau}} da.$$

3. Local kinetics: Large time distribution. In this section, we study the properties of solutions of (2.1)–(2.4). We derive the law of total colony biomass increase, and we show that for both models A and B there exists an asymptotic value for the ratio of the swarm and swimmer cell population densities. This means that, for $z(t) = \frac{u(t)}{v(t)}$, (2.1)–(2.4) result in simple dynamics that have an attracting fixed point. This property will be useful in the analysis of the consolidation phase in section 6. The reader interested in the full diffusion problem should turn to section 4.

3.1. Model A. The analysis of Model A begins by reducing the coupled system (2.1)–(2.2) to a single differential-difference equation for v . We assume that at the start the colony cell population consists of swimmer cells only. This corresponds to the following initial conditions for (2.1)–(2.3):

$$(3.1) \quad v(0) = v_0 > 0 \quad \text{and} \quad q(0, a) \equiv 0, \quad a \in [0, \infty).$$

First, we plug (2.4) into (2.2),

$$(3.2) \quad v'(t) = \frac{1-\xi}{\tau}v(t) + \int_0^t \delta(a-\Theta)q(t, a)e^{\frac{a}{\tau}} da = \frac{1-\xi}{\tau}v(t) + q(t, \Theta)e^{\frac{\Theta}{\tau}}, \quad t > \Theta.$$

Then we use the method of characteristics to solve (2.1) for $q(t, a)$, and in particular $q(t, \Theta)$.

We fix $a \geq 0$ and $t \geq a$ and integrate (2.1) along characteristics. For this, we let $p(s) = q(t+s, a+s)$. Then $q(t, a) - q(t-a, 0) = p(0) - p(-a) = \int_{-a}^0 p'(s)ds$. Hence, because $p'(s) = q_t(t+s, a+s) + q_a(t+s, a+s)$, (2.1) and (2.4) imply

$$q(t, a) - q(t-a, 0) = - \int_{-a}^0 \mu(a)q(t+s, a+s)ds = - \int_{-a}^0 \delta(a-\Theta)q(t+s, a+s)ds.$$

Thus, by (2.5), we obtain

$$(3.3) \quad q(t, a) - q(t-a, 0) = \begin{cases} 0, & a \leq \Theta, \\ -q(t-a+\Theta, \Theta), & a > \Theta. \end{cases}$$

The first lines of (3.3) and (2.3) yield

$$(3.4) \quad q(t, a) = \frac{\xi}{\tau}v(t-a), \quad a \leq \min\{t, \Theta\}.$$

Moreover, by the first line of (3.3),

$$(3.5) \quad q(t-a+\Theta, \Theta) = q(t-a, 0).$$

The combination of (3.3)–(3.5) gives the result

$$(3.6) \quad q(t, a) = \begin{cases} \frac{\xi}{\tau}v(t-a), & a \leq \min\{t, \Theta\}, \\ 0, & a > \Theta. \end{cases}$$

Hence, using (3.6) to replace $q(t, \Theta)$ in (3.2), we obtain an equation for v ,

$$(3.7) \quad v'(t) = \frac{1-\xi}{\tau}v(t) + \frac{\xi}{\tau}v(t-\Theta)e^{\frac{\Theta}{\tau}}, \quad t > \Theta.$$

Equation (3.7) and the initial data

$$(3.8) \quad v(t) = v_0 e^{\frac{1-\xi}{\tau}t}, \quad 0 \leq t \leq \Theta,$$

form an IVP for v .

Remark. The solution of (3.7)–(3.8) on each interval $(n\Theta, (n+1)\Theta]$, $n=1, 2, 3, \dots$, can be calculated recursively using induction on n :

$$v(n\Theta + s) = v_0 e^{\frac{1-\xi}{\tau}s} \sum_{k=0}^n v((n-k)\Theta) \frac{(s\nu)^k}{k!} \quad \text{or}$$

$$v(n\Theta + s) = v_0 e^{\frac{1-\xi}{\tau}s} \sum_{k=0}^n \left[v(n\Theta) + \int_0^s v((n-1)\Theta + \eta) d\eta \right], \quad 0 < s \leq \Theta.$$

The next lemma gives us the law of total biomass increase.

LEMMA 3.1.

$$(3.9) \quad v(t) + u(t) = v_0 e^{\frac{t}{\tau}}.$$

Proof. See Appendix A.

Now we turn to establish an asymptotic formula for $\frac{u}{v}$.

PROPOSITION 3.2. *If $d \equiv \xi(e^{\frac{\Theta}{\tau}} - 1) < 1$, the solution of the IVP (2.1)–(2.6), (3.1) satisfies the following asymptotic relation:*

$$(3.10) \quad \lim_{t \rightarrow \infty} \frac{u(t)}{v(t)} = \frac{\xi\Theta}{\tau}.$$

Proof. Suppose $x(t)$ is a solution of the integral equation

$$(3.11) \quad A[x(t)] = \left(1 + \frac{\xi\Theta}{\tau}\right) e^{\frac{t}{\tau}}, \quad \text{where } A[x(t)] \equiv x(t) + \frac{\xi}{\tau} \int_0^\Theta x(t-a) e^{\frac{a}{\tau}} da.$$

Then

$$x(t) - e^{\frac{t}{\tau}} = \frac{\xi}{\tau} \int_0^\Theta \left\{ e^{\frac{t}{\tau}} - x(t-a) e^{\frac{a}{\tau}} \right\} da = \frac{\xi}{\tau} \int_0^\Theta e^{\frac{a}{\tau}} \left\{ e^{\frac{t-a}{\tau}} - x(t-a) \right\} da.$$

Therefore, taking out a bound on the term in braces and integrating the remaining exponential factor, we get

$$\left| x(t) - e^{\frac{t}{\tau}} \right| \leq d \max_{a \in [0, \Theta]} \left| x(t-a) - e^{\frac{t-a}{\tau}} \right|, \quad t \geq a.$$

This implies

$$\max_{t \in [n\Theta, (n+1)\Theta]} \left| x(t) - e^{\frac{t}{\tau}} \right| \leq d^n \max_{\eta \in [0, \Theta]} \left| x(\eta) - e^{\frac{\eta}{\tau}} \right|,$$

and if $d < 1$, then we have

$$(3.12) \quad \lim_{t \rightarrow \infty} \left| x(t) - e^{\frac{t}{\tau}} \right| = 0.$$

Using (2.8), (3.6), and (3.9), we see that $v(t)$ solves $A[v(t)] = v_0 e^{\frac{t}{\tau}}$, where A is defined in (3.11). Therefore, $y(t) \equiv v_0^{-1} \left(1 + \frac{\xi\Theta}{\tau}\right) v(t)$ satisfies (3.11). If $d < 1$, (3.12) implies

$$(3.13) \quad \lim_{t \rightarrow \infty} y(t) e^{-\frac{t}{\tau}} = 1.$$

Since $v(t) = v_0 y(t) \left(1 + \frac{\xi\Theta}{\tau}\right)^{-1}$, we conclude from (3.13) that

$$(3.14) \quad \lim_{t \rightarrow \infty} \frac{v(t)}{v_0 e^{\frac{t}{\tau}}} = \left(1 + \frac{\xi\Theta}{\tau}\right)^{-1}.$$

Finally, (3.10) follows from (3.14) and (3.9). \square

3.2. Model B. In this subsection, we show that the law of total biomass increase and the asymptotic relation for the cell population densities, properties already established for Model A, hold for Model B as well.

We multiply (2.1) by $e^{\frac{a}{\tau}}$ and integrate with respect to a from 0 to $+\infty$:

$$(3.15) \quad \int_0^\infty q_t(t, a)e^{\frac{a}{\tau}} da + \int_0^\infty q_a(t, a)e^{\frac{a}{\tau}} da + \Theta^{-1} \int_0^\infty q(t, a)e^{\frac{a}{\tau}} da = 0.$$

Applying the Leibnitz rule to the first integral, integrating by parts on the second integral in (3.15), and taking into account (2.6), we have

$$(3.16) \quad u'(t) + q(t, a)e^{\frac{a}{\tau}}|_{a=0}^\infty - \tau^{-1} \int_0^\infty q(t, a)e^{\frac{a}{\tau}} da + \Theta^{-1}u(t) = 0.$$

Finally, we rewrite (3.16), using (2.3), (2.6), and (2.7):

$$(3.17) \quad u'(t) = \frac{\xi}{\tau}v(t) + \left(\frac{1}{\tau} - \frac{1}{\Theta}\right)u(t).$$

Equations (3.17) and (2.2) form a system of differential equations for u and v . For convenience, we state (2.2) again;

$$(3.18) \quad v'(t) = \frac{1-\xi}{\tau}v(t) + \frac{1}{\Theta}u(t).$$

From (3.17) and (3.18) we now derive statements analogous to those given in Lemma 3.1 and Proposition 3.2 of the previous subsection for Model A. Exponential growth of the total biomass follows directly by adding (3.17) and (3.18), since the fact that $(u(t) + v(t))' = \frac{1}{\tau}(u(t) + v(t))$ and (3.1) together imply $u(t) + v(t) = v_0 e^{\frac{t}{\tau}}$.

Now we derive an ODE for $z(t) = \frac{u(t)}{v(t)}$. Plugging the expressions (3.17) and (3.18) for u' and v' in the quotient rule derivative formula for z' yields

$$z' = f(z) \equiv -\frac{1}{\Theta} \left(z^2 + \left(1 - \frac{\xi\Theta}{\tau} \right) z - \frac{\xi\Theta}{\tau} \right).$$

The roots of f are -1 and $\frac{\xi\Theta}{\tau}$. The latter is an attracting fixed point for all nonnegative initial conditions. Thus, for Model B we have $\lim_{t \rightarrow \infty} \frac{u(t)}{v(t)} = \frac{\xi\Theta}{\tau}$.

4. Formulating the population dynamics problem with diffusion. Adding spatial dependence to the population characteristics u and v , we consider the following diffusion problem with kinetics corresponding to (2.1)–(2.3):

$$(4.1) \quad q_t(x, a, t) + q_a(x, a, t) + \mu(a)q(x, a, t) = (D(u, v)q_x(x, a, t))_x,$$

$$(4.2) \quad v_t(x, t) = \frac{1-\xi}{\tau}v(x, t) + \int_0^t q(x, a, t)e^{\frac{a}{\tau}}\mu(a)da,$$

$$(4.3) \quad u(x, t) = \int_0^\infty q(x, a, t)e^{\frac{a}{\tau}}da,$$

$$(4.4) \quad q(x, 0, t) = \frac{\xi}{\tau}v(x, t),$$

$$(4.5) \quad v(x, 0) = g(x) \geq 0, \quad q(x, a, 0) \equiv 0,$$

where $x \in \mathbb{R}$, $t \geq 0$, $0 < a < \infty$. In modeling swarm cell migration, we follow the general framework of age-dependent dispersal. For a detailed discussion of diffusion

problems in the context of age-dependent population models see [13, 21] and references cited there. We take the diffusion coefficient $D(u, v)$ to be density dependent; see (1.2). We shall be more specific about its form below. As before we shall consider two models depending on the form of $\mu(a)$ given in (2.6).

Taking $\mu(a)$ in the form corresponding to Model A, we multiply (4.1) by $e^{\frac{a}{\tau}}$ and integrate over the ages from 0 to ∞ ,

$$(4.6) \quad \int_0^\infty q_t e^{\frac{a}{\tau}} da = - \int_0^\infty q_a e^{\frac{a}{\tau}} da - \int_0^\infty \delta(a - \Theta) q e^{\frac{a}{\tau}} da + \left(D \int_0^\infty q_x e^{\frac{a}{\tau}} da \right)_x.$$

Integration by parts on the first term on the right-hand side of (4.6) yields

$$\int_0^\infty q_t(x, a, t) e^{\frac{a}{\tau}} da = q(x, 0, t) + \frac{1}{\tau} \int_0^\infty q(x, a, t) e^{\frac{a}{\tau}} da - q(x, \Theta, t) e^{\frac{\Theta}{\tau}} + (D(u, v) u_x(x, t))_x.$$

Taking into account (4.3) and (4.4), we have the final equation for u in Model A,

$$(4.7) \quad u_t(x, t) = \frac{1}{\tau} u(x, t) + \frac{\xi}{\tau} v(x, t) - q(x, \Theta, t) e^{\frac{\Theta}{\tau}} + (D(u, v) u_x(x, t))_x.$$

The formulation of Model A is then completed by using (2.4) to rewrite (4.2):

$$(4.8) \quad v_t(x, t) = \frac{1 - \xi}{\tau} v(x, t) + q(x, \Theta, t) e^{\frac{\Theta}{\tau}}.$$

Similarly, for Model B we have

$$(4.9) \quad u_t(x, t) = \left(\frac{1}{\tau} - \frac{1}{\Theta} \right) u(x, t) + \frac{\xi}{\tau} v(x, t) + (D(u, v) u_x(x, t))_x,$$

$$(4.10) \quad v_t(x, t) = \frac{1}{\Theta} u(x, t) + \left(\frac{1}{\tau} - \frac{\xi}{\tau} \right) v(x, t).$$

Hence, for Model B we have obtained the IVP for a parabolic PDE coupled with an ODE. The problem is now in terms of u and v and does not involve the age structure.

Model A can be transformed into Model B via averaging. In (4.7), (4.8), we replace $q(t, \Theta, x) e^{\frac{\Theta}{\tau}}$ by average value $\frac{1}{\Theta} \int_0^\Theta q(x, a, t) e^{\frac{a}{\tau}} da = \frac{1}{\Theta} u(x, t)$. This directly yields (4.9) and (4.10), respectively. Therefore, from now on we shall concentrate on the study of Model B only.

Introducing nondimensional quantities α, μ , and ν , which are equal, respectively, to τ^{-1}, Θ^{-1} , and $\xi \tau^{-1}$, we rewrite (4.9), (4.10) as

$$(4.11) \quad u_t(x, t) = \nu v(x, t) + (\alpha - \mu) u(x, t) + (D(u, v) u_x(x, t))_x,$$

$$(4.12) \quad v_t(x, t) = (\alpha - \nu) v(x, t) + \mu u(x, t).$$

Now, as remarked in the introduction, we choose the diffusion coefficient $D(u, v)$ to have the following form:

$$(4.13) \quad D(u, v) = \frac{D_0 u}{u + kv},$$

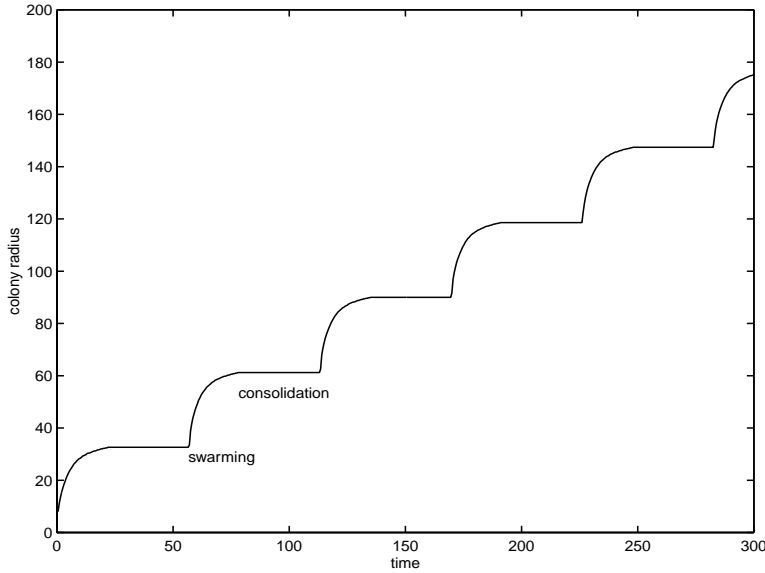


FIG. 1. *The radius versus time plot of the colony expansion. The plotted data reflect the evolution of the size of the spatial support of the solution functions of the IVP for (4.11)–(4.13). The values of parameters are $D_0 = 1$, $k = 5$, $\alpha = 0.7$, $\mu = \nu = 0.6$, $\bar{v} = 12$, and $\tilde{v} = 16$.*

where D_0 and k are positive constants. With this choice, the diffusion coefficient at a given point is a weighted ratio of the spatial density of the swarm cell population to the sum of the spatial densities of the swimmer and swarm cell populations at that point. Thus diffusion is faster in the regions where the ratio of swimmers to the total number of swimmers and swarmers is higher. We also note that the analysis of section 6 applies to a much larger class of nonlinear diffusivities, $D(u, v)$.

We also assume that there is a saturation concentration \tilde{v} of the swimmer cell population above which colony development stops. Therefore, we take the colony development characteristics α, μ , and ν to be continuous functions of v and be equal to 0 when $v > \tilde{v}$. Furthermore, $\alpha(v) \equiv \alpha = \text{const}$ and $\mu(v) \equiv \mu = \text{const}$, when $v < \tilde{v} - \sigma$, for some sufficiently small $\sigma > 0$. Similarly, we define the differentiation factor $\nu(v)$ as a continuous function, which is equal to a positive constant ν on $(\bar{v} + \sigma, \tilde{v} - \sigma)$, and is equal to 0 outside the interval (\bar{v}, \tilde{v}) . Here, the parameter \bar{v} is some real positive number less than $\tilde{v} - 2\sigma$. The differentiation factor of this form ensures that on the new territories, where initially the concentration of swimmers is low, no new swarm cells are produced. This agrees with an observation, found, e.g., in [28], that during consolidation the swimmer cells start producing swarm cells “after a period of time that depends on the culture conditions.”

5. Results from numerical simulations. This section contains a discussion of the results of numerical study of (4.11)–(4.13). The IVP for (4.11)–(4.13) with initial conditions (4.5) was integrated numerically using the explicit Euler finite-difference scheme.

Figure 1 shows how the colony radius changes in time. Here we can see that after some lag period the colony expansion occurs periodically in time. We stopped computing after we had observed several complete cycles of the colony development (Figure 1). In each of these cycles we distinguish two phases, fast colony expansion,

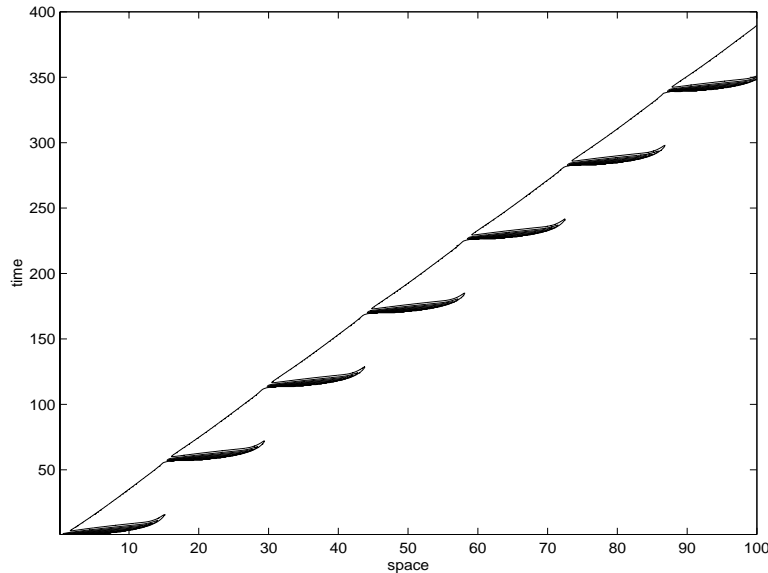


FIG. 2. The contour plot for the diffusion coefficient D . It contains 10 levels in the range between 0 and 1. The darker regions of the plot have dense distribution of the level curves. Away from these regions the diffusion coefficient is small inside the colony boundaries and is zero outside. The comparison with Figure 1 shows that the fast colony expansions coincide in time with the periods of increased diffusivity.

followed by a period in which the colony radius stays unchanged. We compare data, presented in Figure 1, with the dynamics of the diffusion coefficient $D(u, v)$. We also refer to D as the diffusivity. The contour plot of $D(u, v)$, given on Figure 2, shows that the fast colony expansions coincide in time with the periods of the increased diffusivity. This correspondence suggests that one way to gain understanding of the periodicity of the colony development is to study the D -dynamics. Below we shall relate two types of behavior of the diffusion coefficient, observed numerically, to the different phases of the colony development. We shall continue to follow this approach in the subsequent sections, where we shall reformulate and study problem (4.11)–(4.13) in terms of some function of diffusivity.

We now turn to a more detailed description of the numerical simulations. Each cycle of the colony evolution can be viewed as a sequence of two events.

The *consolidation phase* is characterized by the negligible colony expansion, compared to the total colony advancement per cycle. Thus, the colony boundaries at this stage can be considered stationary. The behavior of the diffusion coefficient during the consolidation phase may be described as follows. Figure 3 displays D -profiles at five different moments of time. According to this plot, the dynamics of D resemble a traveling wave, moving in the outward radial direction, until it catches up with the colony boundary. Then it changes rapidly, forming a spike profile (Figure 3). We have checked that this scenario was valid for all other consolidation phases in the numerical simulations. We shall provide an explanation for this in section 6 by an asymptotic analysis near the colony boundary at the end of the consolidation phase.

The quick change of the diffusion coefficient, mentioned above, indicates the start of the *swarming phase*. At the beginning the values of the diffusion coefficient near the interface are close to their supremum D_0 . Consequently, the colony expansion is

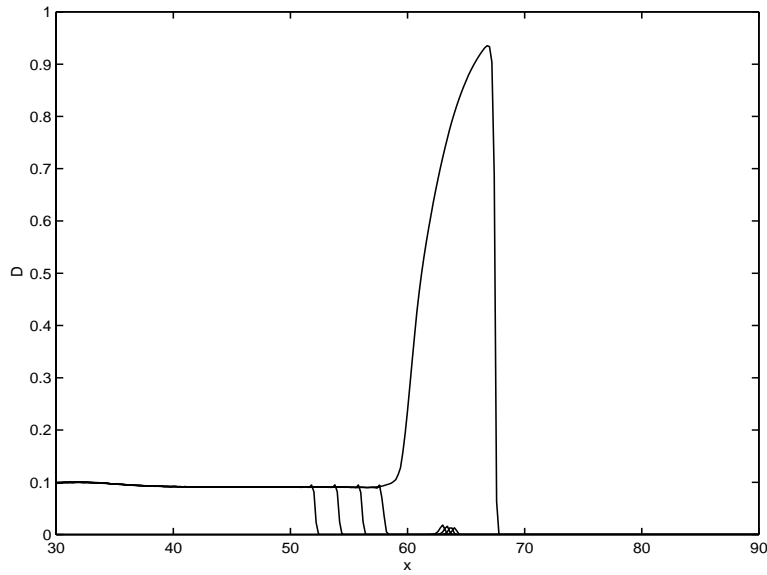


FIG. 3. *The dynamics of the diffusion coefficient $D(u, v)$ during the consolidation phase. The plots of the spatial distribution for D are given at times $t = 98, 102, 106, 110,$ and 114 .*

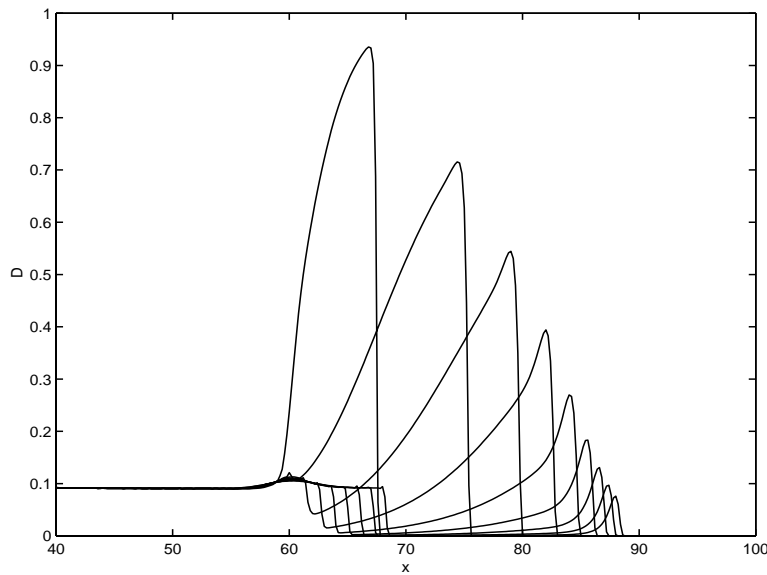


FIG. 4. *The dynamics of the diffusion coefficient $D(u, v)$ during the swarming phase. The plots of the spatial distribution for D are given for moments of time between $t = 114$ and 132 .*

fastest at the start of the swarming phase. Figure 4 shows that, as the colony advances into the new territories, the diffusivity near the interface is gradually decreasing. After some time it gets so small that the change in the colony radius on the scale of the total change per cycle can be neglected. We consider this to be the end of the swarming phase.

Remarkably enough, the dynamics of the diffusion coefficient at the end of the consolidation phase resemble that of the “wave” of cell multiplication in the newly colonized areas observed in the biological experiment at the end of the first consolidation phase. According to [25], this wave begins adjacent to the perimeter of the inoculation spot and spreads outward until it approaches the boundary of the colonized areas. This corresponds to the start of the second swarming phase. There is another reason for which the switch from the consolidation to the swarming phase captures our attention. This is the only distinct event of the whole cycle of the colony development. Indeed, the switch to the swarming phase occurs instantly (Figure 1), while the converse process, a transition to the consolidation phase, takes place over some interval of time. Our study thus focuses on the switch from the consolidation to swarming.

6. Dynamics during the consolidation phase. From (4.11) and (4.12), we derive the equation for $z(x, t) = \frac{u(x, t)}{v(x, t)}$:

$$(6.1) \quad z_t = F(z) + \frac{1}{v} (D(z)(vz)_x)_x, \quad F(z) = (z + 1)(\nu - \mu z),$$

where

$$(6.2) \quad D(z) = \frac{z}{z + k}.$$

Here to simplify notation we took $D_0 = 1$, and we observe that, due to monotonicity of $D(z)$, the dynamics of z fully describe that of D .

Therefore, the system (4.11) and (4.12) can be rewritten as

$$(6.3) \quad z_t = F(z) + \frac{1}{v} (D(z)(vz)_x)_x,$$

$$(6.4) \quad v_t = (\alpha - \nu)v + \mu zv.$$

We shall focus on the dynamics of the diffusion coefficient at the very end of the consolidation phase. According to the numerics, at this time, the wave of diffusivity catches up with the colony boundary, and the diffusion coefficient changes quickly in the neighborhood of the interface (Figure 3). By this we mean that D approaches 1, its least upper bound, while z becomes unbounded. As a result, on the plot of the diffusion coefficient at this moment of time a spike profile appears. The formation of this profile, an event of the consolidation phase, is important for the swarming phase as well, since it gives the z -distribution at the start of the swarming phase.

By means of asymptotic analysis, we shall show that the generation of the spike profile of the diffusion coefficient is effectively the result of the interaction of the traveling front of diffusivity at the end of the consolidation phase and the colony boundary. We have reproduced and studied this effect in the model problems below. In particular, we model the colony boundary by a specifically chosen form of $v(x)$, a static approximation of $v(x, t)$. In fact, the data plotted in Figure 1 suggest that the colony boundary can be considered unchanged for the latter half of the consolidation phase. We explain our choice of the form of $v(x)$ below in this section. It is essential that it has a sharp change about the point x^* , which denotes the colony boundary, and that to the right of x^* , $v(x)$ is small. Otherwise, many different forms of $v(x)$ lead to the formation of a spike profile. We shall see that it is the way $v(x)$ is incorporated

in the diffusion term that is important for the explanation of D -dynamics at the end of the consolidation phase.

In subsection 6.1, we consider the model problem for the linear diffusion case, i.e., $D(z) \equiv 1$. Then in subsection 6.2 we treat the model problem with density-dependent diffusivity, i.e., $D(z)$ given by (1.2).

6.1. Model problem: Linear diffusion. For a first model problem, we simplify the diffusion to be linear, replace the kinetic term with a simpler function, and make a static approximation for $v(x, t)$. In particular, we consider the IVP

$$(6.5) \quad z_t = f(z) + \frac{1}{v} (vz)_{xx}, \quad x \in \mathbb{R}, t > 0,$$

$$(6.6) \quad z(x, 0) \equiv \phi(x) = \begin{cases} 1, & x \leq \ell \ll x^*, \\ 0 & \text{otherwise,} \end{cases}$$

where ℓ is some negative constant,

$$(6.7) \quad v(x) \equiv v \left(\frac{x - x^*}{\epsilon} \right) \equiv \frac{A + \alpha}{2} - \frac{A - \alpha}{2} \tanh \left(\frac{x - x^*}{\epsilon} \right),$$

$$(6.8) \quad f(z) = z(1 - z), \quad 0 < \epsilon \ll 1, 0 < \alpha \ll A.$$

The choice of $v(x)$ is motivated by our intention to model the latter part of the consolidation phase. In the limit of $\epsilon \rightarrow 0$ and $\alpha \rightarrow 0$, v tends to the Heaviside-type function $H(x^* - x)$, which we use as a qualitative picture of the colony boundary at x^* . The method of solution generalizes to a wide range of other forms of v and the choice here provides a good illustration for the analysis.

With $v(x)$ a constant function, (6.5) becomes the equation studied by Kolmogorov, Petrovski, and Piskunov (KPP) in [18]. The solution of the KPP equation with any nonnegative, compactly supported initial data not exceeding 1 evolves approaching a traveling wave solution. Away from some $O(\epsilon)$ -neighborhood of x^* , either $v(x) \approx A$, $x < x^*$, or $v(x) \approx \alpha$, $x > x^*$. Thus, if we choose the initial data with support located far enough from x^* on the left, we expect the solution of (6.5)–(6.6) in the form of a traveling front approaching from the left the neighborhood of x^* , where $v(x)$ has an abrupt change. This seems to be the scenario that $z(x, t)$ undergoes in the full problem (6.3)–(6.4) at the second half of the consolidation phase. Indeed, the numerical solution of the IVP for (6.5)–(6.6) plotted at different times in Figure 5 exhibits a high degree of similarity to that of the full problem plotted in Figure 3.

To understand the solution in the vicinity of x^* we use matched asymptotics. We distinguish an $O(\epsilon)$ -wide transition layer about x^* , also referred as the inner problem region (Figure 6). This is the region in which $v(x)$ changes rapidly. Outside the transition layer $v(x) \approx \text{const}$. Thus, in the outer regions, (6.5) can be approximated by the KPP equation

$$(6.9) \quad Z_t = Z_{xx} + Z(1 - Z).$$

To study (6.5) in the transition layer, we introduce the stretched variable

$$\xi = \frac{x - x^*}{\epsilon},$$

and rewrite (6.5) as

$$\epsilon^2 z_t = \epsilon^2 z(1 - z) + \frac{1}{v} (vz)_{\xi\xi}.$$

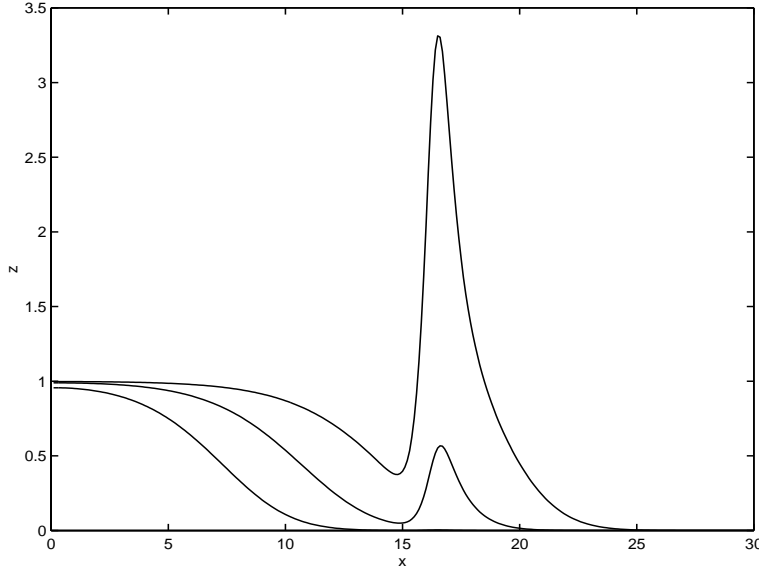


FIG. 5. Model problem (6.5): linear diffusion. The solution profiles are plotted at four moments of time. They reflect the traveling front approaching and then entering the $O(\epsilon)$ -wide neighborhood of $x^* = 15$, where $v(x)$ has a sharp spatial inhomogeneity. The values of other parameters are $\epsilon = 0.5$, $A = 12$, and $\alpha = 0.1$.

The leading order inner problem is now reduced to the ODE

$$(6.10) \quad \frac{1}{v} (vZ)_{\xi\xi} = 0, \quad \text{or, equivalently,} \quad Z_{\xi\xi} + \frac{2v_\xi}{v} Z_\xi + \frac{v_{\xi\xi}}{v} Z = 0.$$

After the expression (6.7) for v , is plugged in (6.10) has the following form:

$$(6.11) \quad Z_{\xi\xi} - a_\delta(\xi) Z_\xi + a_\delta(\xi) \tanh \xi Z = 0,$$

where

$$(6.12) \quad a_\delta(\xi) = \frac{2(1 + \tanh \xi)}{1 + \delta e^\xi \cosh \xi}, \quad 0 < \delta = \frac{A + \alpha}{A - \alpha} - 1 \ll 1.$$

We consider the inner problem as an IVP for (6.10) with dependence on t as a parameter. The initial conditions in ξ are provided by the left outer problem. In turn, the solution of the inner problem at the right edge of the transition layer provides the right outer problem with time-dependent boundary conditions. Thus, in the right outer domain we have an initial boundary value problem.

Matching is assumed to occur at some points x^- and x^+ (Figure 6) and the associated points:

$$\xi^\pm = \frac{x^\pm - x^*}{\epsilon}.$$

The matching conditions are given by

$$(6.13) \quad Z(\xi^-, t) = \mathcal{Z}(x^-, t) \equiv l_0(t),$$

$$(6.14) \quad Z_\xi(\xi^-, t) = \epsilon \mathcal{Z}_x(x^-, t) \equiv \epsilon l_1(t),$$

$$(6.15) \quad \mathcal{Z}(x^+, t) = Z(\xi^+, t), \quad \mathcal{Z}_x(x^+, t) = \frac{1}{\epsilon} Z_\xi(\xi^+, t).$$

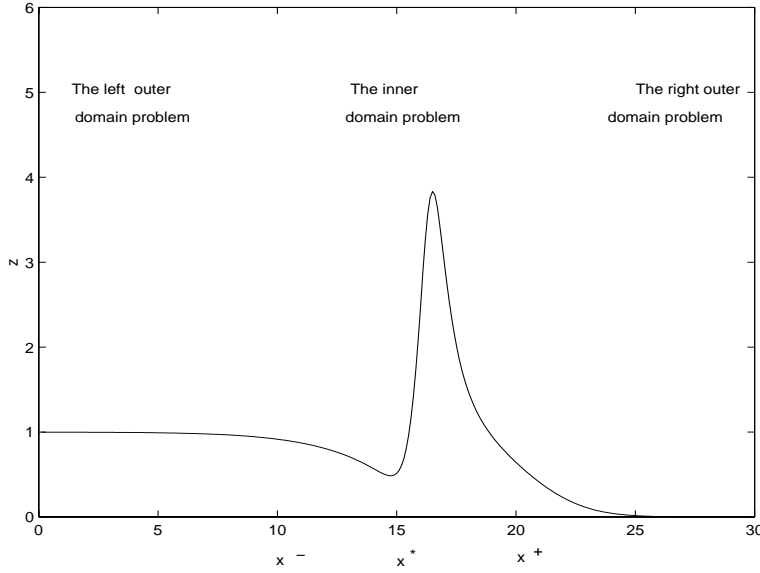


FIG. 6. The inner and outer regions for the IVP (6.5), (6.6).

Here

$$(6.16) \quad 0 \leq l_0(t) \leq 1 \quad \text{and} \quad l_1(t) < 0,$$

because it is known [18] that the solution of the IVP (6.9), (6.6) is uniformly bounded between 0 and 1, and Z_x is negative in the left outer domain. The inner problem now can be formulated as an IVP for (6.10) on the interval (ξ^-, ξ^+) , $\xi^+ - \xi^- = O(\epsilon^{-1})$, with initial conditions (6.13), (6.14). By the maximum principle, the solution of (6.5), (6.6) is nonnegative everywhere and, in particular, in the inner domain. Therefore, we are looking for a nonnegative solution of the IVP for (6.10) with initial conditions (6.13), (6.14).

First, we find the fundamental solution of (6.10):

$$Z^{(1)}(\xi) = e^{-\int_{-\infty}^{\xi} \frac{v}{v} d\tau}, \quad Z^{(2)}(\xi) = \xi e^{-\int_{-\infty}^{\xi} \frac{v}{v} d\tau}.$$

Taking v in the form of (6.7) we have

$$(6.17) \quad Z^{(1)} = 1 + \frac{2e^{2\xi}}{2 + \delta(1 + e^{2\xi})}, \quad Z^{(2)} = \xi \left(1 + \frac{2e^{2\xi}}{2 + \delta(1 + e^{2\xi})} \right).$$

The solution of the inner problem is a linear combination of $Z^{(1)}$ and $Z^{(2)}$,

$$Z(\xi, t) = C_1(t)Z^{(1)}(\xi) + C_2(t)Z^{(2)}(\xi).$$

To determine the unknown coefficients C_1 and C_2 we use the initial conditions (6.13)–(6.14). Plugging $\xi^- = \frac{x^- - x^*}{\epsilon}$ into (6.17), for small $\epsilon > 0$, we compute

$$(6.18) \quad \begin{aligned} Z^{(1)}(\xi^-) &= 1 + \text{EST}, & Z^{(2)}(\xi^-) &= \frac{x^- - x^*}{\epsilon} + \text{EST}, \\ Z_{\xi}^{(1)}(\xi^-) &= 0 + \text{EST}, & Z_{\xi}^{(2)}(\xi^-) &= 1 + \text{EST}, \end{aligned}$$

where EST stands for exponentially small terms. Therefore,

$$(6.19) \quad Z(\xi) = (l_0(t) + l_1(t) (\epsilon\xi - x^- + x^*)) Z^{(1)} + \text{EST}.$$

This explicit formula gives us the desired inner solution in the transition region, and we recall that it satisfies the left matching conditions (6.13) and (6.14) by construction.

We can obtain more information on $l_0(t)$ and $l_1(t)$ as follows. It is well known [18] that the solution of the left outer problem (6.9), (6.6) converges to the traveling wave solution $Z_{tw} = Z_{tw}(x - 2t)$ of (6.9). Therefore, after the period of time necessary for $Z(x, t)$ to get sufficiently close to Z_{tw} , $l_0(t)$ and $l_1(t)$ in (6.19) can be approximated by

$$\tilde{l}_0(t) = Z_{tw}(x^- - 2t) \quad \text{and} \quad \tilde{l}_1(t) = Z'_{tw}(x^- - 2t).$$

The latter values can be read from the phase portrait of the second-order autonomous ODE corresponding to the specified traveling wave solution of (6.9):

$$-2Z'_{tw} = Z''_{tw} + Z_{tw}(1 - Z_{tw}).$$

In particular, the points $(\tilde{l}_0(t), \tilde{l}_1(t))$ lie on the heteroclinic orbit connecting saddle points $(1, 0)$ and $(0, 0)$ in the $Z_{tw} - Z'_{tw}$ phase plane. With $(l_0(t), l_1(t))$ approximated by $(\tilde{l}_0(t), \tilde{l}_1(t))$, (6.19) gives a full description of the inner solution.

Let us now show that the constructed inner solution is consistent with an overall matching scheme. In particular, we want to show that under the initial conditions (6.13)–(6.14) the derivative Z_ξ at ξ^+ is $O(\epsilon)$ in magnitude, so that we can carry out the matching (6.15) with right outer solution. Indeed, only if this condition holds is $Z_x(x^+, t)$ of order $O(1)$, i.e., it does not depend on ϵ , as we expect from the solution in the outer domain.

Noting that $Z_\xi^{(1)}(\pm\infty) = 0$, we use (6.17) to derive

$$\begin{aligned} \frac{Z_\xi(+\infty)}{Z_\xi(-\infty)} &= \frac{Z_\xi^{(2)}(+\infty)}{Z_\xi^{(2)}(-\infty)} = \frac{2 + \delta}{\delta} \quad \text{if } Z_\xi(-\infty) \neq 0, \\ Z_\xi(+\infty) &= 0 \quad \text{otherwise.} \end{aligned}$$

Thus, we have a relationship between the asymptotic values of Z_ξ as $\xi \rightarrow \pm\infty$:

$$(6.20) \quad Z_\xi(+\infty) = \frac{2 + \delta}{\delta} Z_\xi(-\infty).$$

For sufficiently small $\epsilon > 0$, (6.20) and (6.14) imply the desired estimate for $Z_\xi(\xi^+, t)$:

$$(6.21) \quad Z_\xi(\xi^+, t) = \frac{2 + \delta}{\delta} Z_\xi(\xi^-, t) = \frac{2 + \delta}{\delta} l_1(t) \epsilon = O(\epsilon).$$

Note that since $Z_\xi(\xi^-, t)$ is negative according to (6.13) and (6.16), $Z_\xi(\xi^+, t)$ is also negative by (6.21). This agrees with the numerical solution of (6.5)–(6.6) decreasing on the right of the transition layer (Figure 6).

Finally, we estimate the height of the spike h_ϵ for small ϵ by estimating the maximum value of the solution for the limiting $\epsilon = 0$ case. To get a lower bound on h_ϵ , we pick a convenient point for calculation $\xi = \frac{1}{2} \ln\left(\frac{2}{\delta} - 1\right)$ and evaluate (6.19) at $\tilde{\xi}$:

$$Z(\tilde{\xi}) = \left(l_0(t) + l_1(t) \left(\epsilon\tilde{\xi} - x^- + x^* \right) \right) \frac{2 + \delta}{2\delta} + \text{EST}.$$

Taking into account that $\lim_{\epsilon \rightarrow 0} x^- = x^*$, for the limiting height h_0 , we obtain an estimate

$$h_0 = \lim_{\epsilon \rightarrow 0} h_\epsilon \geq \lim_{\epsilon \rightarrow 0} Z(\tilde{\xi}) = \frac{2 + \delta}{2\delta} l_0(t) = O(\delta^{-1}).$$

Hence, for small ϵ , Z grows unbounded as $\delta \rightarrow 0$.

6.2. Model problem: Nonlinear diffusion. Here we continue to study the second half of the consolidation phase. We analyze a model problem with nonlinear diffusion. In particular, we add to the model equation (6.5) a nonlinear diffusion coefficient $D(z)$ (1.2) to obtain an IVP for the following parabolic PDE:

$$(6.22) \quad z_t(x, t) = z(1 - z) + \frac{1}{v} (D(z)(vz)_x)_x,$$

$$(6.23) \quad z(x, 0) = \phi(x),$$

where

$$(6.24) \quad D(z) = \frac{z}{z + k}, \quad k > 0,$$

and the functions $v(x)$ and $\phi(x)$ are as before. The numerical solution of (6.22)–(6.23) is plotted at four different moments of time in Figure 7. As in the case of the model problem with linear diffusion, here we also observe a traveling wave approaching x^* from the left, and this wave changes rapidly in some neighborhood of x^* . However, due to the nonlinear diffusion, the wave profile is qualitatively different from the one studied in the previous subsection. In particular, the solution of (6.22)–(6.23) has its support bounded on the right at any finite time. Our present goal is to extend the matched asymptotic analysis of the previous subsection to take into account the nonlinear diffusion coefficient $D(z)$.

We study the dynamics of the solution of (6.22)–(6.23) starting from the moment when the traveling wave has entered some $O(\epsilon)$ -wide neighborhood of x^* . We use the same matching scheme (6.13)–(6.15) with the following adjustment. For some time, the solution has its support contained in the left outer and the inner domains. Consequently, we do not have to consider the right outer problem until the solution has entered the right outer domain. When the support of the solution extends beyond the inner domain, we must include the right outer problem and the matching condition (6.15).

In terms of the stretched variable ξ , the inner problem has the following form:

$$(6.25) \quad \frac{1}{v} (D(Z)(vZ)_\xi)_\xi = 0, \quad \text{or}$$

$$D \left\{ Z_{\xi\xi} + \frac{2v\xi}{v} Z_\xi + \frac{v\xi\xi}{v} Z \right\} + D' Z_\xi \left\{ Z_\xi + \frac{v\xi}{v} Z \right\} = 0.$$

As for the case with linear diffusion, we are looking for a nonnegative solution of (6.25) with initial conditions (6.13)–(6.14). First, we note that $Z = Z^{(1)} > 0$ solves (6.25) for any admissible $D(z)$. We shall look for another solution in the form of

$$(6.26) \quad Z(\xi) = \Phi(\xi)Z^{(1)}(\xi).$$

Since we are interested in nonnegative solutions of (6.25), the unknown function Φ has to be nonnegative as well. Plug (6.26) in (6.25) to obtain

$$(6.27) \quad \frac{\Phi_{\xi\xi}}{\Phi_\xi} = -\frac{D'Z_\xi}{D(Z)}.$$

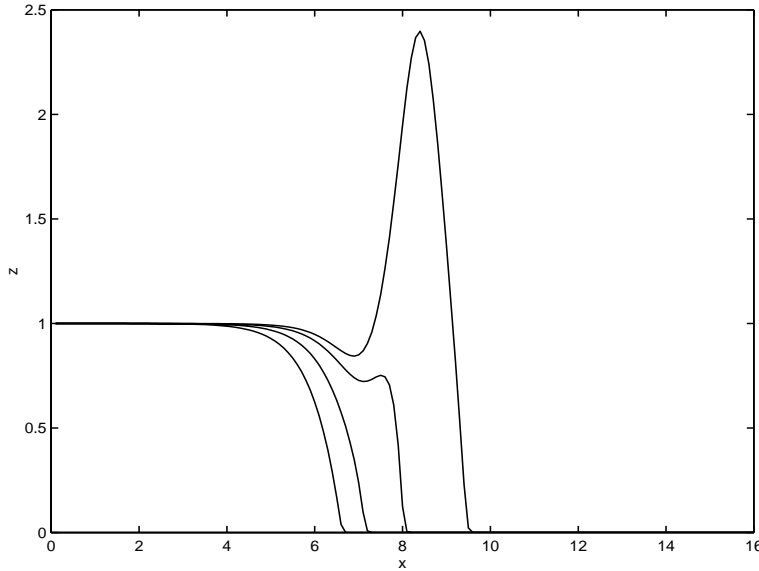


FIG. 7. *Model problem with nonlinear diffusion. The analogous plots to those given on Figure 5 are presented now for the IVP (6.22), (6.24) with nonlinear diffusion. The values of the parameters are $x^* = 7$, $\epsilon = 0.5$, $\alpha = 0.1$, and $A = 12$.*

Integrating (6.27), we have

$$\Phi_\xi = \pm \frac{C_1}{D(Z)}, \quad C_1 \geq 0.$$

Recall that, by (6.17), $Z^{(1)} > 0$ and $Z_\xi^{(1)} \geq 0$. Functions $D(Z)$ and $\Phi(\xi)$ are nonnegative too. Therefore, we have to choose a minus sign and a strictly positive constant C_1 in the formula above; otherwise

$$Z_\xi = \Phi_\xi Z^{(1)} + \Phi Z_\xi^{(1)} \geq 0,$$

which would imply that the inner solution is monotone on the real line, in contradiction to the fact that the numerical solution (Figure 7) is clearly not monotone in the transition layer. Plugging in the expression for the diffusivity (6.24), we obtain

$$(6.28) \quad \Phi_\xi = -C_1 \left(1 + \frac{k}{Z^{(1)}\Phi} \right), \quad C_1 \geq 0.$$

Since, by (6.17), $Z^{(1)}$ is a positive bounded real-valued function, $1 \leq Z^{(1)} \leq 1 + \frac{2}{\delta} = B$, the solution of the IVP for (6.28) at any time will be bounded from below and from above by the solutions of the IVPs for the autonomous ODEs, respectively:

$$\Phi_\xi = -C_1 \left(1 + \frac{C_2}{\Phi} \right), \quad C_2 \in \{k, kB^{-1}\},$$

supplied with the same initial conditions. Therefore, it is sufficient to consider

$$(6.29) \quad \Phi_\xi = -C_1 \left(1 + \frac{C_2}{\Phi} \right).$$

After substitution $y = \Phi^{-1}$ we consider the following IVP:

$$(6.30) \quad y_\xi = C_1 y^2(1 + C_2 y), \quad y(0) = y_0 > 0.$$

Integration of (6.30) yields

$$(6.31) \quad C_1 \xi - C_3 = C_2 \ln \left(C_2 + \frac{1}{y} \right) - \frac{1}{y},$$

where C_3 is an integration constant.

The solution of (6.30) given by (6.31) blows up in finite time. This means that Φ (and, therefore, Z) vanishes at some finite time $\bar{\xi}$. To estimate this time we look at the solution for (6.29), which bounds that of (6.28) from below. Thus, we choose $C_2 = k$ in (6.29):

$$\Phi_\xi = -C_1 \left(1 + \frac{k}{\Phi} \right).$$

In analogy with (6.31), for $\underline{y} = \Phi^{-1}$, we have

$$(6.32) \quad C_1 \xi - C_3 = k \ln \left(k + \frac{1}{\underline{y}} \right) - \frac{1}{\underline{y}}.$$

Now, by plugging $\underline{y} = \infty$ in (6.32), for the time $\underline{\xi}$ of the blow-up of \underline{y} , we obtain

$$\underline{\xi} = \frac{C_3 + k \ln k}{C_1}.$$

Using that $\underline{\Phi} \leq \Phi$ at any time, and that $\underline{\Phi}$ hits zero at $\underline{\xi}$, we obtain a desired estimate for the time $\bar{\xi}$, at which Φ becomes zero:

$$\bar{\xi} \geq \underline{\xi} = \frac{C_3 + k \ln k}{C_1}.$$

The constants C_1 and C_3 are determined from the matching conditions (6.13) and (6.14). We distinguish two cases: (a) $\bar{\xi} = o(\epsilon^{-1})$ and (b) $\bar{\xi} = O(\epsilon^{-1})$. In the first case Z hits zero in the inner domain, excluding the possibility for the matching on the right. This corresponds to the situation of the traveling front in the ϵ -neighborhood of x^* , and there is no right outer problem. Case (b) admits the possibility of matching on the right and is a necessary condition for the right outer problem to exist.

Finally, we show that, as in the case with linear diffusion, the inner solution is unbounded as $\delta \rightarrow 0$. First we note from (6.30) that, in positive time, Φ is uniformly bounded by the initial condition y_0^{-1} from above and by zero from below. This and $\lim_{\delta \rightarrow 0} Z^{(1)} = +\infty$ imply the same limit for the $Z = \Phi Z^{(1)}$.

Remark. We did not use the particular form (6.24) for the diffusion coefficient until (6.28). In fact, the same method can be applied to any other form of diffusivity D , for which (6.22), (6.23) is a well-posed IVP.

To conclude this section, we note that the inner problems for the original equation (6.1) and for the model problem with nonlinear diffusion (6.22) are identical. Therefore, the analysis of the solution of the IVP for (6.22) in the transition layer applies to that of the IVP for (6.1) as well. In particular, the solution of the IVP for (6.1) blows up in the neighborhood of x^* as $\delta \rightarrow 0$. This is what apparently accounts

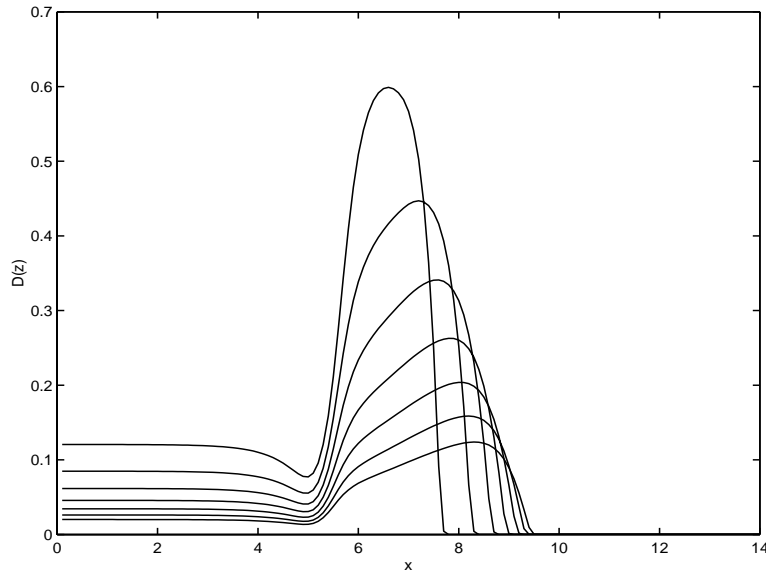


FIG. 8. *The numerical solution to the IVP for (8.2) with the initial conditions as discussed in section 7. Profiles of $D(z)$ are shown at various times, and one sees the front advancing and the maximum of the spike decreasing.*

for the formation of the spike profile of the diffusivity at the end of consolidation phase in the full problem (6.3), (6.4).

7. The swarming phase. In this section, we turn our attention to the events of the swarming phase. The presentation here is more descriptive than formal. We recall briefly what we know about the dynamics of swarming from the simulations discussed in section 5. It starts at the moment when the preceding consolidation phase ends, namely, when the wave of diffusivity has caught up with the colony boundary. The diffusion coefficient exhibits a characteristic spike profile. This spike profile propagates rapidly at the beginning and then gradually slows down until the interface comes almost to rest. Throughout this phase the peak of the wave of diffusivity decreases (Figure 4).

Heuristically, the numerically observed behavior may be explained as follows. At the start, when the swarm cells move into the unoccupied territory just outside the colony boundary, the proportion of them there is high and so is the diffusivity. Thus, the colony expands rapidly. The differentiation factor $\nu(v)$ is zero on the newly colonized areas, where the swimmer cell population density, $v(x, t)$, is below \bar{v} . Hence, no swimmer cells enter the swarm cell development channel. Since swarm cells septate and are not reproduced, the diffusivity decreases and after some time the colony expansion becomes insignificant on the scale of the colony radius increase per cycle.

We now show that this behavior is expected and that the heuristic explanation can be justified by analyzing the governing equations. During the swarming phase, the salient feature is that the swarm cells move onto the newly colonized areas, where for some period of time the swimmer cell population surface density is low. We use this to simplify the original equations. On the new territories we have $\nu(v) = 0$, until the swimmer cell population density builds up to \bar{v} . In addition, taking $\alpha(v) = \mu(v)$

to be equal to constant α for simplicity, we have

$$(7.1) \quad \begin{aligned} u_t &= (D(u, v)u_x)_x, \\ v_t &= \alpha(u + v), \quad D(u, v) = \frac{D_0 u}{u + kv}. \end{aligned}$$

The absence of the reaction terms in (7.1) suggests that on the new territories the swarm cell population density $u(x, t)$ eventually decreases, while the swimmer cell density $v(x, t)$ increases. Therefore, the diffusion coefficient should eventually decrease. To make this argument rigorous we would need estimates of the flux of the swarm cells from the already occupied territories and for the time when the system (7.1) is valid. Unfortunately, these estimates are quite difficult to obtain, despite the plausibility of the solution behavior, and we now take a different approach.

Applying the strategy also followed when analyzing the consolidation phase, we rewrite (7.1) in terms of $z(x, t) = \frac{u(x, t)}{v(x, t)}$:

$$(7.2) \quad \begin{aligned} z_t &= -\alpha z(1 + z) + \frac{1}{v} (D(z)(vz)_x)_x, \\ v_t &= \alpha v(1 + z), \quad D(z) = \frac{D_0 z}{z + k}. \end{aligned}$$

The z - and v -profiles at the end of the consolidation phase serve as initial data for the equations. There, $z(x, t)$ exhibits a spike profile, and the v -distribution may be approximated by the function

$$(7.3) \quad v(x, t^*) = \frac{A + \alpha}{2} - \frac{A - \alpha}{2} \tanh\left(\frac{x - x^*}{\epsilon}\right),$$

where $0 < \alpha \ll A$, and x^* denotes the position of the colony boundary at time t^* , the end of the consolidation phase. The support of $v(x, t^*)$ is chosen to be all of \mathbb{R} , and the values of $v(x, t^*)$ for $x > x^*$ can be made arbitrarily small. We note that this is necessary since, if $v(x, t^*)$ had bounded support, the support would never change due to the form of (7.2 b). Moreover, we note that this is merely an artifact of working with the equations for z and v . If one works instead with the original system for u and v , then one could use the initial data of bounded support.

We numerically integrate (7.2) using the above initial conditions. The results are given in Figure 8. They reproduce the solution dynamics well during the swarming phase in the full problem (Figure 4). Thus, the IVP for (7.2) gives a good approximation to the dynamics of swarming. The scenario of the swarming phase can be roughly described as a translation of the initial z -profile with an accompanying decrease in magnitude due to action of the kinetic part of (7.2). In summary, we have seen that the dynamics of the swarming phase are largely explained by the z -distribution at the end of the preceding consolidation phase.

8. A rigorous justification of the method of section 6. In section 6, we studied the model problems in order to explain the nature of the rapid changes in the solution of (6.3), (6.4) in the transition layer during the consolidation phase. We constructed self-consistent asymptotic solutions in the limit of $\epsilon \rightarrow 0$. The study of these solutions in the transition layer about x^* revealed that they grew unbounded as $\delta \rightarrow 0$, where the small parameter $\delta > 0$ appeared naturally from the definition (6.7) of function v . The goal of this section is a rigorous justification of the asymptotic procedure used in section 6. Moreover, we show that it can be used to construct a

uniformly in time valid approximate solution of (6.5), (6.6) on bounded intervals of the real line for small ϵ .

First, we review the inner and outer problems and the time-dependent matching conditions. Next, we construct a uniformly valid asymptotic solution in the inner and outer domains. At the end of this section we state Theorem 8.3, justifying this construction. In section 9 we give the proof of the Theorem 8.3.

8.1. Review of the inner and outer problems for the model problem with linear diffusion. To set up notation convenient for the purposes of these sections, we restate the definitions of the inner and outer problems. Consider an IVP for (6.5), (6.7), where, without loss of generality, we set $x^* = 0$:

$$(8.1) \quad z_t = z(1 - z) + \frac{1}{v} (vz)_{xx}, \quad -\infty < x < +\infty, \quad t > 0,$$

$$(8.2) \quad z(x, 0) = \phi(x),$$

where

$$(8.3) \quad v(x) \equiv v\left(\frac{x}{\epsilon}\right) \equiv \frac{A + \alpha}{2} - \frac{A - \alpha}{2} \tanh\left(\frac{x}{\epsilon}\right), \quad 0 < \alpha \ll A.$$

For simplicity assume that

$$(8.4) \quad \phi(x) = \begin{cases} 1, & x < \ell \ll 0, \\ 0 & \text{otherwise} \end{cases}$$

In the transition layer, where v has a sharp spatial inhomogeneity, we rewrite (8.1) using the inner variable $\xi = \frac{x}{\epsilon}$:

$$(8.5) \quad \epsilon^2 z_t = \epsilon^2 z(1 - z) + \frac{1}{v} (vz)_{\xi\xi}.$$

The leading order inner problem is then

$$(8.6) \quad \frac{1}{v} (vZ)_{\xi\xi} = 0.$$

There are two outer problems, one on each side of the transition layer. Outside some neighborhood of zero, we have $v(x) \approx A$ (when $x < 0$) and $v(x) \approx \alpha$ (when $x > 0$). Thus, in the outer regions, (8.1) can be approximated by the KPP equation:

$$(8.7) \quad Z_t = Z(1 - Z) + Z_{xx}.$$

8.2. Domains of validity and matching. In this section, we define the domains of validity for the inner and outer problems.

DEFINITION 8.1. *By a domain of validity of the inner problem we mean an interval $I^\epsilon = (x_\ell, x_r)$, such that*

$$\limsup_{\epsilon \rightarrow 0} \sup_{x \in I^\epsilon} \left| Z\left(\frac{x}{\epsilon}, t\right) - z(x, t) \right| = 0, \quad t \geq 0,$$

provided $Z(\xi_\ell, t) = z(x_\ell, t)$ and $Z_\xi(\xi_r, t) = \epsilon z_x(x_r, t)$, where $\xi_\ell = \frac{x_\ell}{\epsilon}$.

We concentrate on the left outer problem and matching of the left outer solution with the solution of the inner problem (recall (6.13) and (6.14)). The analysis for the right outer problem can be done in complete analogy with that for the left outer domain. We shall comment on it at the end of this section. For the rest of this section and in the one that follows, unless specifically mentioned otherwise, by the outer problem (solution) we mean the left outer problem (solution).

Similarly, we define a domain of validity of the outer problem.

DEFINITION 8.2. *By a domain of validity of the outer problem we mean an interval \mathcal{I}^ϵ such that*

$$\limsup_{\epsilon \rightarrow 0} \sup_{x \in \mathcal{I}^\epsilon} |\mathcal{Z}(x, t) - z(x, t)| = 0, \quad t \geq 0,$$

where \mathcal{Z} and z are solutions of the IVPs for (8.7) and (8.1), respectively, with the same initial conditions (8.2).

Remark. The intervals I^ϵ and \mathcal{I}^ϵ do not depend on t .

In their respective domains of validity, the inner and outer asymptotic solutions can be considered as approximations of $z(x, t)$ that are uniform in t for $t \geq 0$ and small ϵ . Suppose now that an overlap domain $J = I^\epsilon \cap \mathcal{I}^\epsilon$ is not empty. Choose an arbitrary point $x^- \in J$. We continue the outer solution through the inner domain by assigning the initial conditions at $\xi^- = \frac{x^-}{\epsilon}$:

$$(8.8) \quad Z(\xi^-, t) = \mathcal{Z}(x^-, t),$$

$$(8.9) \quad Z_\xi(\xi^-, t) = \epsilon \mathcal{Z}_x(x^-, t).$$

Then we define a uniformly valid asymptotic solution in the inner and outer domains to be

$$(8.10) \quad z_{asympt}(x, t) = \begin{cases} \mathcal{Z}(x, t), & (-\infty, x^-] \cap \mathcal{I}^\epsilon, \\ Z\left(\frac{x}{\epsilon}, t\right), & (x^-, \infty) \cap I^\epsilon. \end{cases}$$

In section 9, we prove the following theorem for $z_{asympt}(x, t)$.

THEOREM 8.3. *Let $z(x, t)$ be a solution of the IVP (8.1)–(8.4). Then there exist nonempty inner and left outer domains of validity, I^ϵ and \mathcal{I}^ϵ (in the sense of Definitions 8.1 and 8.2). Although the left outer domain is assumed to be of a finite size, it can be extended arbitrarily far to the left. Moreover, for $\epsilon > 0$ small enough, the overlap domain $J \equiv I^\epsilon \cap \mathcal{I}^\epsilon$ is nonempty, and, for any $x^- \in J$,*

$$z(x, t) \rightarrow z_{asympt}(x, t), \quad x \in I^\epsilon \cup \mathcal{I}^\epsilon, t > 0,$$

uniformly, as $\epsilon \rightarrow 0$.

Remark. A symmetric argument gives the same statement for the right outer domain. We do not present the analysis for the right outer domain since it can be done in exactly the same way as that of this section and section 9 and since we are primarily interested in the front dynamics before and within the transition layer.

9. Proof of Theorem 8.3. The goal of this section is to prove Theorem 8.3. Subsection 9.1 contains some preliminary estimates for the solution of (8.1)–(8.4). In subsection 9.2, we establish the domain of validity of the inner problem and estimate the difference between the asymptotic and exact solutions therein. This difference has

two components: one is due to the reduction to the leading order equation and the other is due to the error in the initial conditions at ξ^- . At this step we are concerned with the first component only. Next, in subsection 9.3, we determine the domain of validity for the outer problem and show that the overlap domain between the inner and outer domains is not empty. Then we use the estimates of accuracy of the outer solution to determine the bounds for the second component of the difference between the exact and the asymptotic solutions, namely for the error in the initial conditions for the inner problem. After this we go back, in subsection 9.4, to the inner domain and estimate the composite error. This analysis will show the uniform convergence of the exact solution of (8.1)–(8.4) to the asymptotic one, as $\epsilon \rightarrow 0$, in the left outer and inner domains. The main tools used are a priori estimates and comparison theorems for parabolic equations.

9.1. A priori estimates. In the course of the proof we will be working with several IVPs for semilinear parabolic PDEs of the type

$$u_t - Lu = F(x, t, u(x, t)),$$

where L is a uniformly elliptic linear differential operator with smooth coefficients. The existence of a classical solution in each case will follow from the results of [18]. For more general results, we refer to [12, 19].

We start a proof of convergence by deriving from Lemmas 9.1 and 9.3 some auxiliary estimates for the solution of (8.1)–(8.4). The goal here is to obtain bounds on the solutions and their derivatives that are independent of ϵ .

LEMMA 9.1. *Let z be a solution of the IVP (8.1)–(8.4). Then there exists $C_1 > 0$ such that*

$$|z(x, t)| < C_1, \quad -\infty < x < +\infty, t \geq 0.$$

The constant C_1 does not depend on ϵ .

Here and below, C with and without subscripts will denote various different constants, independent of ϵ . We shall allow for some of the C 's to stand for different constants. The meaning of each of them should be clear from the context.

Proof. Note that $z \equiv 0$ is a subsolution for (8.1)–(8.4). Therefore, we need only show that $z(x, t)$ is bounded from above.

In fact, the function $\max\{1, \tilde{z}(x, t)\}$ is a supersolution, provided \tilde{z} satisfies (8.2) and

$$(9.1) \quad \tilde{z}_t = \frac{1}{v} (v\tilde{z})_{xx}, \quad -\infty < x < +\infty, t > 0.$$

To show this, suppose $\tilde{z} > 1$; otherwise, the constant function 1 is a supersolution. Then

$$\tilde{z}_t - \tilde{z}(1 - \tilde{z}) - \frac{1}{v} (v\tilde{z})_{xx} = -\tilde{z}(1 - \tilde{z}) > 0.$$

It remains to show that $\tilde{z}(x, t)$ is bounded on the real line uniformly in t , so that the solution of (8.1)–(8.4) is, as well. We change variables in (9.1) to

$$\xi = \frac{x}{\epsilon}, \quad \tau = \epsilon^{-2}t, \quad \text{and} \quad \tilde{z} = w e^{-\int_{-\infty}^{\xi} \frac{v'}{v} d\eta}.$$

This results in

$$w_\tau = w_{\xi\xi}.$$

Hence, there exists a constant W such that

$$|w(\xi, \tau)| \leq W, \quad -\infty < \xi < +\infty, \tau \geq 0,$$

and it follows that

$$|\tilde{z}(x, t)| \leq W \sup_{\xi} e^{-\int_{\xi_0}^{\xi} \frac{v'}{v} d\eta} \leq \left(1 + \frac{2}{\delta}\right) W, \quad -\infty < x < +\infty, t \geq 0.$$

This proves the lemma. \square

Next we give well-known derivative estimates, obtained from the Schauder estimates for parabolic PDEs [12]. Since we will refer to them several times, for convenience, we state these results here following [12, 19, 9].

Let Q be a rectangle $(x_0, x_1) \times (t_0, t_1)$ in (x, t) plane, where $-\infty < x_0 < x_1 < \infty$ and $-\infty < t_0 < t_1 < \infty$. Corresponding to Q and to a number $\gamma > 0$, let Q_{γ} be a smaller rectangle $[x_0 + \gamma, x_1 - \gamma] \times [t_0 + \gamma, t_1]$. For a function u sufficiently smooth in Q , let

$$|u|_0^Q \equiv \sup_{(x,t) \in Q} |u(x, t)|, \quad |u|_1^Q \equiv |u|_0^Q + |u_x|_0^Q, \quad |u|_2^Q \equiv |u|_1^Q + |u_{xx}|_0^Q + |u_t|_0^Q.$$

THEOREM 9.2. *Let $u_t - u_{xx} = h(x, t)$ in Q , where $h(x, t)$ is a continuous function in \bar{Q} . Then for some $C > 0$, not depending on u and h ,*

$$(9.2) \quad |u|_1^{Q_{\gamma}} \leq C \left(|h|_0^Q + |u|_0^Q \right).$$

Furthermore, if h_x exists in Q , then

$$(9.3) \quad |u|_2^{Q_{\gamma}} \leq C \left(|h|_1^Q + |u|_0^Q \right).$$

LEMMA 9.3. *Let z be a solution of the IVP (8.1)–(8.4) and D_{α} denote a spatial domain $(-m, -M\epsilon^{1-\alpha}) \cup (M\epsilon^{1-\alpha}, m)$ for arbitrary fixed $M > 0, m > 0$, and $\alpha > 0$. Then for a given $T > 0$,*

$$(a) \quad \exists C_1 > 0 : |z|_2^{Q_1} \leq C_1, \quad Q_1 \equiv D_{\alpha} \times [\gamma, T], \quad \gamma > 0,$$

$$(b) \quad \exists C_2, C_3 > 0 : \int_c^d |z_t| dx \leq C_2 + C_3(d - c), \quad t \geq 0, \quad c < d.$$

Proof. First, we change the dependent variable in (8.1),

$$(9.4) \quad z(x, t) = B(x)y(x, t),$$

where

$$(9.5) \quad B(x) = e^{-\int_{-\infty}^x \frac{v_x(\eta)}{v(\eta)} d\eta} = 1 + \frac{2e^{\frac{2x}{\epsilon}}}{2 + \delta \left(1 + e^{\frac{2x}{\epsilon}}\right)}.$$

Substituting (9.4) into (8.1) and (8.3) yields an equivalent IVP for y :

$$(9.6) \quad y_t = y_{xx} + h(x, t), \quad h(x, t) \equiv y(1 - B(x)y),$$

$$y(x, 0) = B^{-1}(x)\phi(x).$$

Note that

$$(9.7) \quad 1 \leq B(x) \leq 1 + \frac{2}{\delta}.$$

This and Lemma 9.1 imply

$$(9.8) \quad |h(x, t)| \leq C_4, \quad x \in \mathbb{R}, t \geq 0.$$

Using (9.2), (9.8), and Lemma 9.1, we obtain a bound on $|y_x|$:

$$(9.9) \quad |y|_1^Q \leq C_5, \quad Q = [-m, m] \times [\gamma, T], \gamma > 0.$$

The constant C_5 does not depend on ϵ .

By direct estimation in (9.5), we have

$$(9.10) \quad |B'(x)|, |B''(x)| \leq C_6, \quad x \in D_\alpha,$$

where C_6 does not depend on ϵ . Therefore, (9.8)–(9.10) imply

$$(9.11) \quad |h|_1^{Q_2} \leq C_7, \quad Q_2 \equiv D_\alpha \times [\gamma, T], \quad \gamma > 0,$$

and C_7 does not depend on ϵ . Finally, (9.11) and Lemma 9.1 together enable us to use (9.3) and obtain a bound on $|y|_2^{Q_1}$ independent of ϵ :

$$(9.12) \quad |y|_2^{Q_1} \leq C_8 \left(|h|_1^{Q_2} + |y|_0^Q \right) \leq C_9, \quad Q_1 \equiv D_\alpha \times [\gamma, \infty), \quad \gamma > 0.$$

The constant C_9 does not depend on ϵ .

Part (a) of the lemma follows immediately from (9.4), (9.10), and (9.12).

To prove part (b), we multiply (9.6) by a smooth test function w and integrate by parts over (c, d) :

$$(9.13) \quad \int_c^d y_t w dx = y_x w \Big|_c^d - \int_c^d y_x w_x dx - \int_c^d h(x, t) w dx.$$

Without loss of generality we can assume that y_t does not change the sign of (c, d) , since otherwise we can divide (c, d) into subintervals, where y_t does not change the sign and for each of them repeat the same argument. Choosing w in (9.13), such that $w \equiv \text{sign}(y_t(x, t))$ on (c, d) , we have

$$(9.14) \quad \int_c^d |y_t| dx = \text{sign}(w) \left(y_x(d, t) - y_x(c, t) - \int_c^d h(x, t) dx \right).$$

Applying (9.8) and (9.9) to (9.14), we obtain

$$(9.15) \quad \int_c^d |y_t| dx \leq C_2 + C_3(d - c),$$

where C_2 and C_3 do not depend on ϵ . The statement of part (b) follows from (9.4), (9.8), and (9.15). \square

9.2. The size of the inner domain of validity. The size of the inner domain of validity is given by the following lemma.

LEMMA 9.4. *The size of the domain of validity of the inner problem is of order $o(1)$ as $\epsilon \rightarrow 0$.*

Proof. Subtracting (8.6) from (8.5) we obtain a differential equation for the difference $y(\xi, t) = z(\epsilon\xi, t) - Z(\xi, t)$:

$$(9.16) \quad y_{\xi\xi} + 2\frac{v'}{v}y_{\xi} + \frac{v''}{v}y = \epsilon^2g(\xi, t), \quad g(\xi, t) \equiv z_t(\epsilon\xi, t) - z(1 - z).$$

We want to estimate the maximum size of $I^\epsilon = (x_\ell, x_r)$ such that

$$\lim_{\epsilon \rightarrow 0} \sup_{x \in I^\epsilon} \left| y\left(\frac{x}{\epsilon}, t\right) \right| = 0, \quad t \geq 0,$$

provided

$$(9.17) \quad y(\xi_\ell, t) = y_\xi(\xi_\ell, t) = 0, \quad \xi_\ell = \frac{x_\ell}{\epsilon}.$$

The general solution of (9.16) is

$$(9.18) \quad y(\xi, t) = D_1Z^{(1)}(\xi) + D_2Z^{(2)}(\xi) + \epsilon^2 \int_{\xi_\ell}^{\xi} K(\xi, s)g(s, t)ds,$$

where $Z^{(1)}(\xi)$ and $Z^{(2)}(\xi)$ are given by (6.17) and

$$K(\xi, s) = \frac{Z^{(1)}(\xi)}{Z^{(1)}(s)}(\xi - s).$$

From (9.17) and (6.18), we have first that $D_1 = 0 + \text{EST}$ and then also $D_2 = 0 + \text{EST}$. Therefore,

$$(9.19) \quad y(\xi, t) = \epsilon^2 \int_{\xi_\ell}^{\xi} K(\xi, s)g(s, t)ds = \epsilon^2 Z^{(1)}(\xi) \int_{\xi_\ell}^{\xi} \frac{g(s, t)}{Z^{(1)}(s)}(\xi - s)ds.$$

It is easily seen from (6.17) that $Z^{(1)}$ is bounded by constants $1 \leq Z^{(1)} \leq 1 + \frac{2}{\delta}$, independent of ϵ . This allows us to derive the following bound:

$$(9.20) \quad |y(\xi, t)| \leq \epsilon^2 C (\xi_r - \xi_\ell) \int_{\xi_\ell}^{\xi_r} |g(s, t)| dt, \quad \xi \in (\xi_\ell, \xi_r).$$

By part (b) of Lemma 9.3, the right-hand side of (9.20) will tend to zero as $\epsilon \rightarrow 0$, provided $\xi_r - \xi_\ell = o(\epsilon^{-1})$. This gives us the desired estimate of the size of the inner domain of validity:

$$|I^\epsilon| = x_r - x_\ell = \epsilon(\xi_r - \xi_\ell) = o(1). \quad \square$$

9.3. The size of the outer domain of validity. Our next step is to obtain similar estimates for the outer domain. This is done by showing, first, in Lemma 9.5 that the asymptotic solution is a supersolution for (8.1)–(8.4) in the outer domain. Then the difference between the exact solution and the asymptotic solution can be estimated by constructing a subsolution and comparing it to the asymptotic solution. This is achieved in Lemmas 9.6–9.8.

LEMMA 9.5. *For $\epsilon > 0$ sufficiently small, the solution of (8.7) with initial condition given by (8.2) is a supersolution for (8.1)–(8.4) on the negative semiaxis.*

Proof. Rewrite (8.1) as follows:

$$(9.21) \quad Lz = 0, \quad \text{where} \quad Lz \equiv z_t - z(1 - z) - z_{xx} - 2\frac{v'}{v}z_x - \frac{v''}{v}z.$$

Let $-\infty < a_1 < a_2 < 0$ and $\gamma > 0$. Then there exist positive constants C_1 and C_2 such that

$$(9.22) \quad 0 < C_1 \leq \mathcal{Z}(x, t) \quad \text{and} \quad -\infty < C_2 \leq \mathcal{Z}_x(x, t) < 0 \quad \text{in} \quad (a_1, 0] \times [\gamma, +\infty).$$

Here $\mathcal{Z}(x, t)$ continues to denote the solution of (8.7), (8.2). The estimates in (9.22) can be derived from well-known properties of the solution of (8.7), (8.2) [18].

It can be verified directly by differentiating in (8.3) that there exists a positive constant V such that

$$(9.23) \quad -\frac{A - \alpha}{\epsilon} \leq v'(x) \leq 0, \quad -\infty < x < +\infty,$$

$$(9.24) \quad v''(x) \leq -\frac{V}{\epsilon^2}, \quad a_1 \leq x \leq a_2.$$

Using (8.7), we evaluate

$$L\mathcal{Z} = -2\frac{v'}{v}\mathcal{Z}_x - \frac{v''}{v}\mathcal{Z}.$$

Therefore, from (9.22)–(9.24) and the fact that $v(x) > 0$ by (8.3), we conclude that for $\epsilon > 0$ sufficiently small

$$L\mathcal{Z} > 0, \quad -\infty < a_1 \leq x \leq a_2 < 0, \quad t \geq \gamma > 0.$$

This proves the lemma. \square

Now we turn to constructing a subsolution for (8.1)–(8.4). For this, we introduce an auxiliary IVP:

$$(9.25) \quad w_t = w(1 - b_\epsilon - w) + w_{xx}, \quad -\infty < x < +\infty, t > 0,$$

$$(9.26) \quad w(x, 0) = \begin{cases} 1 - b_\epsilon, & x < \underline{\ell}, \\ 0 & \text{otherwise,} \end{cases}$$

where

$$(9.27) \quad b_\epsilon = -\psi(-M\epsilon^{-1+\alpha}),$$

function ψ is defined as $\frac{v''}{v}$, $M > 0$ and $\underline{\ell}$ are arbitrary constants, and $0 < \alpha < 1$. Note that, using (6.12), ψ can also be written as

$$(9.28) \quad \psi(\xi) = a_\delta(\xi) \tanh \xi.$$

LEMMA 9.6. *For $\epsilon > 0$ sufficiently small, the solution of the IVP (9.25), (9.26) is a subsolution for (8.1)–(8.4) on the interval $(-\infty, -M\epsilon^{1-\alpha})$, $0 < \alpha < 1$, provided $w(x, 0) \leq \phi(x)$ (i.e., $\underline{\ell} \leq \ell$).*

Proof. We want to show that $Lw \leq 0$, where the differential operator L was introduced in (9.21). First, we rewrite (9.21) as follows:

$$(9.29) \quad Lw = w_t - w_{xx} - w(1 - b_\epsilon - w) - b_\epsilon w - \frac{2v'}{v}w_x - \frac{v''}{v}w.$$

Using (9.25), (9.29) can be reduced to

$$(9.30) \quad Lw = - \left(b_\epsilon + \frac{v''}{v} \right) w - \frac{2v'}{v}w_x.$$

It is known that $w_x \leq 0$ [18]. This and (9.23) allow us to derive from (9.30)

$$(9.31) \quad Lw \leq w \left(\psi(-M\epsilon^{-1+\alpha}) - \psi\left(\frac{x}{\epsilon}\right) \right), \quad 0 < \alpha < 1.$$

As follows from (9.28) and (6.12), $\psi(\xi)$ is decreasing for negative values of ξ , that are far enough away from the origin. This and $w \geq 0$ imply in (9.31) that, for $\epsilon > 0$ sufficiently small, $Lw \leq 0$, provided

$$\frac{x}{\epsilon} \leq -M\epsilon^{-1+\alpha}.$$

The statement of the lemma therefore follows. \square

Now we are in a position to construct a subsolution for (8.1)–(8.4) on the interval $(-\infty, -M\epsilon^{1-\alpha})$. We introduce a function

$$\underline{z}(x, t) = (1 - b_\epsilon) \mathcal{Z} \left(\sqrt{1 - b_\epsilon}x, (1 - b_\epsilon)t \right),$$

where \mathcal{Z} is a solution of (8.7) that satisfies the initial conditions given by (8.4).

LEMMA 9.7. *For $\epsilon > 0$ sufficiently small, \underline{z} is a subsolution for (8.1)–(8.4) on the interval $(-\infty, -M\epsilon^{1-\alpha})$.*

Proof. We note that \underline{z} satisfies (9.25) and

$$\underline{z}(x, 0) = \begin{cases} 1 - b_\epsilon, & x < \frac{\ell}{\sqrt{1 - b_\epsilon}}, \\ 0 & \text{otherwise.} \end{cases}$$

Since $0 < b_\epsilon < 1$, $\underline{z}(x, 0) \leq \phi(x)$. Now Lemma 9.6 implies that, for $\epsilon > 0$ sufficiently small, $\underline{z}(x, t)$ is the desired subsolution. This completes the proof of the lemma. \square

The super- and subsolutions constructed in Lemmas 9.5 and 9.7 can be used to estimate the difference between the exact solution $z(x, t)$ and its asymptotic approximation $\mathcal{Z}(x, t)$ in the outer domain. From these estimates we will be able to determine the size of the *outer domain of validity*. We will restrict our attention to the left outer domains bounded on the left, e.g., by an arbitrary sufficiently large in absolute value negative constant m . This does not affect the range of applicability of the asymptotic scheme since it was intended to help understanding of the solution behavior in the regions adjacent to the transition layer and in the transition layer. It also simplifies the analysis.

LEMMA 9.8. *For $\epsilon > 0$ sufficiently small,*

$$0 \leq \mathcal{Z}(x, t) - z(x, t) \leq C e^{-2M\epsilon^{-1+\alpha}}, \quad x \in (-m, -M\epsilon^{1-\alpha}), \quad t \geq 0 \quad \forall \alpha \in (0, 1),$$

where constant C does not depend on ϵ .

Proof. By the comparison principle, the solution of (8.1)–(8.4) is known to be bounded [18]:

$$0 < \mathcal{Z}(x, t) < 1, \quad x \in (-\infty, \infty), \quad t \geq 0.$$

Then a priori estimates, given in Theorem 9.2, imply that for any positive m and T there exists a constant $L > 0$ such that

$$(9.32) \quad |\mathcal{Z}_x(x, t)|, |\mathcal{Z}_{xx}(x, t)|, |\mathcal{Z}_t(x, t)| \leq L \quad x \in (-m, m), \quad \gamma \leq t \leq T.$$

Applying Lemmas 9.5 and 9.7, for $x \in (-m, -M\epsilon^{1-\alpha})$, $0 < \alpha < 1$, and $t \geq 0$, we have

$$(9.33) \quad \underline{z}(x, t) = (1 - b_\epsilon) \mathcal{Z}(\sqrt{1 - b_\epsilon}x, (1 - b_\epsilon)t) \leq z(x, t) \leq \mathcal{Z}(x, t).$$

Thus, for $x \in (-m, -M\epsilon^{1-\alpha})$ and $t \geq 0$,

$$(9.34) \quad 0 \leq \mathcal{Z}(x, t) - z(x, t) \leq \left| \mathcal{Z}(x, t) - \mathcal{Z}(\sqrt{1 - b_\epsilon}x, (1 - b_\epsilon)t) \right| + b_\epsilon \left| \mathcal{Z}(\sqrt{1 - b_\epsilon}x, (1 - b_\epsilon)t) \right|.$$

First, we show that the statement of the lemma is valid on any finite time interval $[0, T]$, $0 < T < \infty$. Using (9.34) and by restricting t to $[0, T]$, for $x \in (-m, -M\epsilon^{1-\alpha})$ we have

$$(9.35) \quad \left| \mathcal{Z}(x, t) - \mathcal{Z}(\sqrt{1 - b_\epsilon}x, (1 - b_\epsilon)t) \right| \leq \left| \mathcal{Z}(x, t) - \mathcal{Z}(\sqrt{1 - b_\epsilon}x, t) \right| + \left| \mathcal{Z}(\sqrt{1 - b_\epsilon}x, t) - \mathcal{Z}(\sqrt{1 - b_\epsilon}x, (1 - b_\epsilon)t) \right| \leq Lm(1 - \sqrt{1 - b_\epsilon}) + LTb_\epsilon.$$

Since $b_\epsilon \rightarrow 0$ as $\epsilon \rightarrow 0$, for small $\epsilon > 0$, $1 - \sqrt{1 - b_\epsilon} \leq b_\epsilon$. Plugging this into the last inequality, for $x \in (-m, -M\epsilon^{1-\alpha})$, we obtain

$$(9.36) \quad \left| \mathcal{Z}(x, t) - \mathcal{Z}(\sqrt{1 - b_\epsilon}x, (1 - b_\epsilon)t) \right| \leq L(m + T)b_\epsilon, \quad t \in (0, T).$$

Combining (9.34) and (9.36), we get

$$0 \leq \mathcal{Z}(x, t) - z(x, t) \leq C_1 b_\epsilon, \quad x \in (-m, -M\epsilon^{1-\alpha}), t \in (0, T),$$

where constant $C_1 = 2L(m + T) + 1$, does not depend on ϵ . Furthermore, from (9.27), (9.28), and (6.12) it can be easily seen that for some positive C_2

$$(9.37) \quad |b_\epsilon| \leq C_2 e^{-2M\epsilon^{-1+\alpha}}.$$

Therefore,

$$0 \leq \mathcal{Z}(x, t) - z(x, t) \leq C e^{-2M\epsilon^{-1+\alpha}}, x \in (-m, -M\epsilon^{1-\alpha}), t \in (0, T).$$

To complete the proof for all positive times $t > 0$, we use the well-known fact [18] that

$\mathcal{Z}(x, t)$ and $\underline{\mathcal{Z}}(x, t)$ converge in time for constant functions 1 and $1 - b_\epsilon$, respectively, uniformly in x on bounded intervals. Therefore, for sufficiently large $T > 0$ and $t \geq T$, from (9.33) follows

$$0 \leq \mathcal{Z}(x, t) - z(x, t) \leq \mathcal{Z}(x, t) - \underline{\mathcal{Z}}(x, t) \leq 2b_\epsilon \leq 2C_2 e^{-2M\epsilon^{-1+\alpha}},$$

$$x \in (-m, -M\epsilon^{1-\alpha}). \quad \square$$

COROLLARY 9.9. For $\epsilon > 0$ sufficiently small,

$$|\mathcal{Z}_x(x, t) - z_x(x, t)| \leq \epsilon^\beta, \quad x \in (-m, -M\epsilon^{1-\alpha}), t > 0, 0 < \alpha < 1, \beta > 0.$$

Proof. The proof will be by contradiction. Suppose that for some $\beta > 0$, $x_0 \in (l, -M\epsilon^{1-\alpha})$, and $t_0 > 0$,

$$\mathcal{Z}_x(x_0, t_0) - z_x(x_0, t_0) > 4C\epsilon^\beta,$$

where the positive constant C does not depend on ϵ . Then, as follows from part (a) of Lemma 9.3 and estimates in (9.31), there exists a constant $C_1 > 0$ that does not depend on ϵ and such that the following holds. Let $\eta = C_1\epsilon^\beta$, then $x_0 + 2\eta < M\epsilon^{1-\alpha}$ and

$$\mathcal{Z}_x(x, t_0) - z_x(x, t_0) > 2C\epsilon^\beta, \quad x \in (x_0, x_0 + 2\eta).$$

Thus,

$$z(x_0 + \eta, t_0) - \mathcal{Z}(x_0 + \eta, t_0) = z(x_0, t_0) - \mathcal{Z}(x_0, t_0) + \int_{x_0}^{x_0 + \eta} z_x(x, t_0) - \mathcal{Z}_x(x, t_0) d\xi$$

$$(9.38) \quad \geq z(x_0, t_0) - \mathcal{Z}(x_0, t_0) + 2C\eta\epsilon^\beta = z(x_0, t_0) - \mathcal{Z}(x_0, t_0) + 2CC_1\epsilon^{2\beta}.$$

Next, we apply Lemma 9.8 to (9.38) to obtain that, for sufficiently small $\epsilon > 0$,

$$z(x_0 + \eta, t_0) - \mathcal{Z}(x_0 + \eta, t_0) \geq CC_1\epsilon^{2\beta} > 0.$$

Here, we get a contradiction to Lemma 9.8 and, therefore, for $\epsilon > 0$ small enough,

$$(9.39) \quad z_x(x, t) - \mathcal{Z}_x(x, t) \leq \frac{\epsilon^\beta}{2}, \quad x \in (-m, -M\epsilon^{1-\alpha}), t > 0, 0 < \alpha < 1, \beta > 0.$$

In complete analogy with (9.39), we can show that

$$(9.40) \quad \underline{\mathcal{Z}}_x(x, t) - z_x(x, t) \leq \frac{\epsilon^\beta}{2}, \quad x \in (-m, -M\epsilon^{1-\alpha}), t > 0, 0 < \alpha < 1, \beta > 0,$$

provided that $\epsilon > 0$ is small. Combining (9.39) and (9.40) and substituting into them the expression for $\underline{\mathcal{Z}}(x, t)$, we obtain

$$(9.41) \quad (1 - b_\epsilon)^{\frac{3}{2}} \mathcal{Z}_1 \left(\sqrt{1 - b_\epsilon} x, (1 - b_\epsilon)t \right) - \frac{\epsilon^\beta}{2} \leq z_x(x, t) \leq \mathcal{Z}_x(x, t) + \frac{\epsilon^\beta}{2},$$

where \mathcal{Z}_1 denotes a partial derivative with respect to the first argument. Taking into account (9.38), after a straightforward estimation procedure eliminating b_ϵ from (9.41), we finally have

$$|z_x(x, t) - \mathcal{Z}_x(x, t)| \leq \epsilon^\beta, \quad x \in (-m, -M\epsilon^{1-\alpha}), t > 0.$$

This proves the corollary. \square

Remark. In the outer domain, we have used the derivatives estimates, which depend on the size of the time domain (Theorem 9.2). However, the specific property of the solutions of the IVP for (8.7) with certain initial conditions that they converge to 1 uniformly on bounded intervals allows us to obtain uniform in time estimates in Lemma 9.8, Corollary 9.9, and Theorem 8.3.

9.4. The end of the proof of Theorem 8.3. From Lemma 9.8, it follows that the left outer domain of validity, \mathcal{I}^ϵ , extends to the right up to $-M\epsilon^{1-\alpha}$, $\alpha > 0$. Here we use the notation of Lemma 9.8. According to Lemma 9.4, the inner domain of validity I^ϵ is located about the origin and is $o(1)$ in size. Therefore, the overlap domain $J = I^\epsilon \cap \mathcal{I}^\epsilon$ is nonempty. We can construct the approximate solution $z_{asympt}(x, t)$ in the inner and outer domains, as it was described at the end of section 8. Our task is to estimate the difference $|z(x, t) - z_{asympt}(x, t)|$ in $I^\epsilon \cup \mathcal{I}^\epsilon$ and $t > 0$ and to show that it goes to zero uniformly as $\epsilon \rightarrow 0$. To do so we combine the results, given in the Lemmas 9.4 and 9.8, taking into account the error in the inner region due to the matching (8.8), (8.9). The initial conditions for the inner problem are given by the outer solution and, therefore, contain some error. We will show that this component of the error is of a higher order than that already estimated in Lemma 9.4. Thus it affects neither the size of the inner domain of validity nor the accuracy of the asymptotic solution.

The equation for the error is given by (9.16). In contrast to (9.17), we have to consider the solution of (9.16) satisfying the following nontrivial initial conditions:

$$(9.42) \quad y(\xi^-, t) = z(\epsilon\xi^-, t) - \mathcal{Z}(\epsilon\xi^-, t) \equiv e_0,$$

$$(9.43) \quad y_\xi(\xi^-, t) = \epsilon [z_x(\epsilon\xi^-, t) - \mathcal{Z}_x(\epsilon\xi^-, t)] \equiv e_1.$$

Here, $\xi^- = \frac{x^-}{\epsilon}$, $x^- \in J$, is the point of matching of the inner and outer solutions after rescaling. According to Lemma 9.8 and Corollary 9.9 and using the same notations, for $\epsilon > 0$ sufficiently small,

$$(9.44) \quad |e_0| \leq Ce^{-2M\epsilon^{1-\alpha}}, \quad |e_1| \leq \epsilon^\beta, \quad 0 < \alpha < 1, \beta > 0.$$

Using (9.42) and (9.43), we obtain the system of equations for the unknown coefficients D_1 and D_2 in (9.18):

$$(9.45) \quad \begin{cases} D_1 Z^{(1)}(\xi^-) + D_2 Z^{(2)}(\xi^-) = e_0, \\ D_1 Z_\xi^{(1)}(\xi^-) + D_2 Z_\xi^{(2)}(\xi^-) = e_1. \end{cases}$$

Let us choose ξ^- in the form of $\xi^- = C\epsilon^{-\kappa}$. Since $\xi^- = \frac{x^-}{\epsilon}$ and x^- , by construction, belongs to the overlap domain $J = I^\epsilon \cap \mathcal{I}^\epsilon$, we have the following constraints for κ :

$$(9.46) \quad 0 < \kappa < \alpha < 1.$$

Using the fundamental solution given by (6.17), we estimate the coefficients in (9.45):

$$\begin{aligned}
 (9.47) \quad Z^{(1)}(\xi^-) &= 1 + \frac{2}{2+\delta} e^{-2C\epsilon^{-\kappa}} + \text{HOT (higher order terms)}, \\
 Z^{(2)}(\xi^-) &= -2C\epsilon^{-\kappa} \left(1 + \frac{2}{2+\delta} e^{-2C\epsilon^{-\kappa}} \right) + \text{HOT}, \\
 Z_\xi^{(1)}(\xi^-) &= \frac{4}{2+\delta} e^{-2C\epsilon^{-\kappa}} + \text{HOT}, \\
 Z_\xi^{(2)}(\xi^-) &= 1 + \frac{2e^{-2C\epsilon^{-\kappa}}}{2+\delta} (1 - 2C\epsilon^{-\kappa}) + \text{HOT}.
 \end{aligned}$$

Applying the rule of Kramer to the system (9.45) and taking into account the estimates (9.44) and (9.47), we obtain the estimates for the unknown coefficients D_1 and D_2 :

$$(9.48) \quad D_1 = O(\epsilon^{\beta-\kappa}), \quad D_2 = O(\epsilon^\beta).$$

By (9.46), $\kappa < 1$. Then, since β can be taken arbitrarily large, we conclude from (9.18) and (9.48) that the contribution of the first two terms in (9.18) is insignificant compared to the third term. Therefore, the error associated with the initial conditions in the inner problem does not affect the size of the inner domain of validity, established on the basis of (9.20) in Lemma 9.4. Thus, we have proven Theorem 8.3, justifying the asymptotic scheme constructed in section 6.

10. Discussion. In the present paper, we used a reaction-diffusion system to model and analyze the formation of spatial patterns in *Proteus mirabilis* bacterial colonies. For the reaction part, we took the equations of local kinetics based on the assumptions on the cell-differentiation mechanism in *Proteus mirabilis* that were derived by Esipov and Shapiro [8]. Unlike the model in [8], our treatment of diffusion uses only density-dependent colony characteristics without explicit dependence on age structure. The model contains only four parameters: the rate of growth, the rate of septation, the differentiation factor, and the diffusion coefficient. All of them are density dependent. The functional forms of the parameters are rather simple and based only on the robust colony properties observed experimentally.

The models we created were shown numerically to have periodic colony front dynamics and alternation of phases of the colony development, just as seen in the biological experiments and in the Esipov-Shapiro model [8]. Thus, we conclude that the explicit age dependence in the system parameters is not necessary for the robust periodicity of the colony evolution.

The model suggests a scenario for the switch between the consolidation and swarming phases. According to this scenario, we predict during the second half of the consolidation phase a wave of diffusivity inside the colony that travels in the outward radial direction. A new swarming phase starts when this wave has caught up with the colony boundary. This is consonant with colony dynamics observed experimentally [25] for the first consolidation phase. While the periodicity and the waves of diffusivity were found numerically, our main focus was to investigate analytically the switch from the consolidation phase to the swarming phase, the culmination of the colony development cycle.

The periodic character of the colony evolution and the resultant concentric ring patterns found for *Proteus mirabilis* is not an isolated phenomenon. Periodicity and similar patterns were also reported for the colonies formed by another bacteria, *Bacillus subtilis* [22]. The observations made on the *Bacillus subtilis* colonies resemble those

for *Proteus mirabilis*. In particular, short cells can differentiate to form elongated and flagellated multicellular forms that can move across semisolid agar surfaces. Macroscopically, under certain conditions *Bacillus subtilis* colonies undergo consolidation and swarming phases in alternation, just as in the *Proteus mirabilis* case. Internal density waves that were reported for *Proteus* [25], are also present in the *Bacillus subtilis* colonies [24]. Thus, colony development of both species have many common features.

Bacillus subtilis colonies can exhibit a number of different spatial patterns for different environmental conditions [22, 24] (e.g., agar and nutrient concentrations). Among other patterns, in [22] Matsushita studied the formation mechanism for the disk-like patterns resulting from the colony homogeneously spreading. The experimental data reported in [22] is consistent with the traveling wave dynamics derived from a population dynamics model (i.e., a reaction-diffusion equation). However, as stated in [22, 24], patterns with periodic front dynamics pose a more complicated modeling question. The model that we developed and studied in this paper provides an example of periodic front dynamics in the framework of reaction-diffusion systems.

Finally, besides *Proteus mirabilis* and *Bacillus subtilis*, there are other species (e.g., *Escherichia coli* and *Salmonella typhimurium*) that combine the ability to move across semisolid surfaces and cell differentiation. Thus, reaction-diffusion systems give a natural framework for studying the dynamics of such systems and resultant spatial patterns.

Appendix A. Proof of Lemma 3.1. First, we derive a simple relation, which we shall need later in the proof. Integrating $p'(s) = \frac{\partial}{\partial s}q(t+s, a+s)$ from $-\Delta$ to 0, in complete analogy to the derivation of (3.2), we obtain

$$q(t, a) = q(t - \Delta, a - \Delta) \quad \text{for } 0 \leq \Delta \leq a \leq \min\{t, \Theta\}.$$

This implies

$$q(t - \alpha, \beta) = q(t - \alpha - (\beta - \alpha), \beta - (\beta - \alpha))$$

and, hence,

$$(A.1) \quad q(t - \alpha, \beta) = q(t - \beta, \alpha), \quad 0 \leq \alpha, \beta \leq \min\{t, \Theta\}.$$

Next, we verify (3.8) for $t \in (0, \Theta]$. For this, we rewrite (2.1), (2.2) with account to (2.3) for $0 < a, t \leq \Theta$,

$$(A.2) \quad q_t(t, a) + q_a(t, a) = 0,$$

$$(A.3) \quad v'(t) = \frac{1 - \xi}{\tau} v(t).$$

From (A.3) and (3.1), we obtain

$$(A.4) \quad v(t) = v_0 e^{\frac{1-\xi}{\tau} t}.$$

Using (A.4) and (3.5), we integrate (A.2)

$$(A.5) \quad q(t, a) = \begin{cases} q(t - a, 0) = \frac{\xi}{\tau} v(t - a) = \frac{\xi}{\tau} v_0 e^{\frac{1-\xi}{\tau}(t-a)}, & 0 < a \leq t \leq \Theta, \\ 0, & 0 < t < a \leq \Theta. \end{cases}$$

We use (A.5) to compute

$$u(t) = \frac{\xi}{\tau} v_0 \int_0^t e^{\frac{1-\xi}{\tau}(t-a)} e^{\frac{a}{\tau}} da = v_0 e^{\frac{t}{\tau}} - v(t).$$

Thus,

$$(A.6) \quad v(t) + u(t) = v_0 e^{\frac{t}{\tau}},$$

and the lemma is proven for $t \in (0, \Theta]$. We now turn to establish the same result for $t > \Theta$.

Using (3.5), we integrate by parts in the expression (2.5) for $t > \Theta$:

$$u(t) = \frac{\xi}{\tau} \int_0^\Theta v(t-a) e^{\frac{a}{\tau}} da = \xi \left\{ e^{\frac{\Theta}{\tau}} v(t-\Theta) - v(t) + \int_0^\Theta v'(t-a) e^{\frac{a}{\tau}} da \right\}.$$

Using (2.2), we get

$$u(t) = \xi \left\{ e^{\frac{\Theta}{\tau}} v(t-\Theta) - v(t) + \frac{1-\xi}{\tau} \int_0^\Theta v(t-a) e^{\frac{a}{\tau}} da + \int_0^\Theta \left[\int_0^{t-a} \mu(\eta) q(t-a, \eta) e^{\frac{\eta}{\tau}} d\eta \right] e^{\frac{a}{\tau}} da \right\}.$$

Now straightforward calculation shows

$$(A.7) \quad u(t) = \xi \left\{ e^{\frac{\Theta}{\tau}} v(t-\Theta) - v(t) + (1-\xi)u(t) + I \right\},$$

where, using (A.2) and (2.5),

$$(A.8) \quad I = e^{\frac{\Theta}{\tau}} \int_0^\Theta q(t-a, \Theta) e^{\frac{a}{\tau}} da = e^{\frac{\Theta}{\tau}} \int_0^\Theta q(t-\Theta, a) e^{\frac{a}{\tau}} da = e^{\frac{\Theta}{\tau}} u(t-\Theta).$$

We rewrite (A.7), taking (A.8) into account:

$$(A.9) \quad u(t) + v(t) = e^{\frac{\Theta}{\tau}} (u(t-\Theta) + v(t-\Theta)), \quad t > \Theta.$$

Hence, the assertion of the lemma also holds for $t > \Theta$, and the proof is complete.

Acknowledgments. We are grateful to J. Shapiro for introducing us to this subject; we thank Shapiro and S. Esipov for helpful conversations and for providing us with preprints of their manuscripts. T. Kaper also thanks O. Diekmann for a useful conversation.

REFERENCES

[1] B.P. AYATI, *A Variable Time Step Method for an Age-Dependent Population Model with Non-linear Diffusion*, preprint, Univ. Chicago, Computer Science Department, 1998.
 [2] R. BELAS, *Proteus mirabilis and other swarming bacteria*, in *Bacteria as Multicellular Organisms*, J.A. Shapiro and M. Dworkin, eds., Oxford University Press, New York, 1997.
 [3] M.P. BRENNER, L.S. LEVITOV, AND E.O. BUDRENE, *Physical mechanisms for chemotactic pattern formation by bacteria*, *Biophysical J.*, 74 (1998), pp. 1677–1693.
 [4] N.F. BRITTON, *Reaction-Diffusion Equations and Their Applications to Biology*, Academic Press, London, 1986.

- [5] C. CHIU, F.C. HOPPENSTEADT, AND W. JAGER, *Analysis and computer simulation of accretion patterns in bacterial cultures*, J. Math. Biol., 32 (1994), pp. 841–855.
- [6] O. DIEKMANN, *Thresholds and travelling waves for the geographical spread of infection*, J. Math. Biol., 6 (1978), pp. 110–130.
- [7] W. ECKHAUS, *Matched Asymptotic Expansions and Singular Perturbations*, North-Holland, Amsterdam, 1973.
- [8] S.E. ESİPOV AND J.A. SHAPIRO, *Kinetic model of Proteus mirabilis swarm colony development*, J. Math. Biol., 36 (1998), pp. 249–268.
- [9] P.C. FIFE, *Mathematical Aspects of Reacting and Diffusing Systems*, Lecture Notes in Biomath. 28, Springer-Verlag, Berlin, New York, 1979.
- [10] P.C. FIFE, *Dynamics of Internal Layers and Interfaces*, SIAM, Philadelphia, 1988.
- [11] P.C. FIFE AND L.HSIAO, *The generation and propagation of internal layers*, Nonlinear Anal., 12 (1988), pp. 19–41.
- [12] A. FRIEDMAN *Partial Differential Equations of Parabolic Type*, Prentice-Hall, Englewood Cliffs, NJ, 1964.
- [13] M.E. GURTIN AND R.C. MACCAMY, *Product solutions and asymptotic behavior for age-dependent, dispersing populations*, Math. Biosci., 62 (1982), pp. 157–167.
- [14] T. HOFER, J.A. SHERRATT, AND P.K. MAINI, *Dictostelium discodium: Cellular self-organization in an excitable medium*, Proc. Roy. Soc. London Ser. B, 259 (1995), pp. 249–257.
- [15] T. HOFER, J.A. SHERRATT, AND P.K. MAINI, *Cellular pattern formation during Dictostelium aggregation*, Phys. D, 85 (1995), pp. 425–444.
- [16] F.C. HOPPENSTEADT AND W. JAGER *Pattern formation by bacteria*, in Biological Growth and Spread, Lecture Notes in Biomath. 38, Springer-Verlag, Berlin, New York, 1980, pp. 68–81.
- [17] E.F. KELLER AND L.A. SEGEL, *Initiation of slime mold aggregation viewed as an instability*, J. Theor. Biol., 26 (1970), pp. 399–415.
- [18] A.N. KOLMOGOROV, I.G. PETROVSKII, AND N.S. PISCOUNOFF, *A study of the equation of diffusion with increase in the quantity of matter, and its application to a biological problem*, Bjul. Mosk. Gos. Univ., 1 (1937), pp. 1–26; translated in Dynamics of Curved Fronts, P. Pelce, ed., Academic Press, Boston, 1988.
- [19] O.A. LADYZHENSKAYA AND N.N. URALTSEVA, *Linear and Quasilinear Equations of Parabolic Type*, AMS Translations, Providence, RI, 1968.
- [20] P.A. LAGERSTROM, *Matched Asymptotic Expansions: Ideas and Techniques*, Springer-Verlag, New York, 1988.
- [21] R.C. MACCAMY, *A population model with nonlinear diffusion*, J. Differential Equations, 39 (1981), pp. 52–72.
- [22] M. MATSUSHITA, *Formation of colony patterns by a bacterial cell population*, in Bacteria as Multicellular Organisms, J.A. Shapiro and M. Dworkin, eds., Oxford University Press, New York, 1997.
- [23] J.D. MURRAY, *Mathematical Biology*, Springer-Verlag, New York, 1993.
- [24] I. RAFOLS, *Formation of Concentric Rings in Bacterial Colonies*, M.Sc. thesis, Chuo University, Japan, 1998.
- [25] O. RAUPRICH, M. MATSUSHITA, C. J. WELJER, F. SIEGERT, S.E. ESİPOV, AND J.A. SHAPIRO, *Periodic phenomena in Proteus mirabilis swarm colony development*, J. Bacteriology, 178 (1996), pp. 6525–6538.
- [26] J.A. SHAPIRO AND D. TRUBATCH, *Sequential events in bacterial colony morphogenesis*, Phys. D, 49 (1991), pp. 214–223.
- [27] J. SMOLLER, *Shock Waves and Reaction-Diffusion Systems*, Springer-Verlag, New York, 1983.
- [28] F.D. WILLIAMS AND R.H. SCHWARZHOFF, *Nature of the swarming phenomenon in Proteus*, Ann. Rev. Microbiol., 32 (1978), pp. 101–122.
- [29] A.B. VASIL'VA, V.F. BUTUZOV, AND L.V. KALACHEV, *The Boundary Function Method for Singular Perturbation Problems*, SIAM, Philadelphia, 1993.
- [30] A.I. VOLPERT, V.A. VOLPERT, AND V.A. VOLPERT, *Traveling Wave Solutions of Parabolic Systems*, AMS, Providence, RI, 1994.